1-1-2015

Some experimental investigation on effect of light and vibration on nano coated piezo for energy harvesting

Abhay Sharma
University of Mississippi

SOME EXPERIMENTAL INVESTIGATIONS ON EFFECT OF LIGHT AND VIBRATION ON NANOCOATED PIEZO FOR ENERGY HARVESTING

A thesis
presented in partial fulfillment of requirements
for the degree of Master of Science
in the Department of Mechanical Engineering
University of Mississippi

by

Abhay Sharma

December 2015

ABSTRACT

PZT is a promising piezoelectric ceramic material which has a wide range of applications in a variety of fields such as acoustic sensors and transducers, electrical switches, medical instrumentation, artificial sensitive skin in robotics, automotive detection on roads, nondestructive testing , structural health monitoring and as a biocompatible material. In this research a cantilever based multi energy harvester was developed to maximize the power output of PZT sensor. Nano mixtures containing graphene, ferrofluid nanoparticle (FNP) and ZnO nano particles were used to enhance the piezoelectric and photovoltaic output of the sensor. The samples were tested under different energy conditions to observe the behavior of nano coated PZT film under multi energy conditions (vibration and light). Composition of the ZnO and FNP was changed by weight in order to achieve the optimal composition of the nano mixture. Light energy, vibration energy, combined effect of light and vibration energy were used to explore the behavior of the sensor. The sensor with 1% Epoxy, 40% ZnO and 59% FNP achieved a maximum power output of 9404.28 µWatt/sec with vibration only from 65-400Hz. The sensor with 1% Epoxy, 5% graphene 40% ZnO and 54% FNP achieved a maximum power output of 13279.23 µWatt/sec when under the combined effect of light (3780 lumens) and vibration energy (65-400Hz). This was nearly 3 times more power output than the pure PZT sensor.

DEDICATION

I would like to dedicate this thesis to my parents Mr. Bijay Kumar Sharma and Dr. Mrs. Chandrakala Sharma.

ACKNOWLEDGEMENTS

I would first like to express my sincere gratitude towards my advisor Dr. J. P. Sharma, for offering me a chance to work with him. Then I would like to express my sincere gratitude to my co-advisor Dr. Tyrus McCarty, without his knowledge and assistance this study would not have been successful. I also would like to express my deepest appreciation to Dr. A. M. Rajendran, Professor and Chair, Mechanical Engineering Department, for admitting me to the department and his kind financial support. He has been very helpful and was always supportive. I am very grateful to Mrs. Nadeeka Karunarathna, Mr. Matt Lowe and Mr. Dwight O'Dell they have helped a lot in gathering up the materials required for my experiments and guided me about the operation of equipment. I would also like to thank Dr. Raju Mantena who let me use his microscope and his Ph.D. student Damian Stoddard, Dr. Paul Scovazzo for letting me use his Spin coating machine, Dr. John O'Haver for letting me use his AFM machine and his Ph.D. student candidate Pohlee Cheah who assisted me in the operation of AFM. I would also like to thank my friends Mohammad Afrough and Matthew Nelms for their assistance whenever needed. My deepest appreciation should always go to my loving parents and family members for their understanding, sacrifices, and all the support so far in my life.

Last but not least, I thank all of my colleagues for their encouragement and support to complete my studies.

CONTENTS

LIST OF FIGURES

LIST OF TABLES

CHAPTER 1. BACKGROUND RESEARCH

1.1 Introduction

In the existing universe, there is an endless requirement for more energy which simultaneously should be clean and the generation technique should be eco-friendly. This desire was the motivation behind working on renewable energy sources. With renewable energy as the main source of energy in today's world for electricity, we can minimize the issues of global warming and variation in climate. The problem arises with the output power of these energy sources, which is low, unreliable and is not as easy to regulate with the changing demand cycles like the traditional sources of power. To overwhelm this concern properly storing this generated power from renewable energy sources can be a viable option. Hence to count on these sources to be primary sources of energy proper storage is a desired factor.

There is an abundance of solar and wind energy in the surrounding environment. A large portion of this energy is transformed into heat and vibration and is lost into the atmosphere without being used.

1.2 Energy Harvesting

Energy harvesting is the process of scavenging energy from freely available sources like solar power, wind energy, thermal energy, etc. There are many ways of harvesting energy from the environment including solar energy, thermal, photovoltaic, electromagnetic and vibration based devices. Every method has its own constraints like solar methods require sufficient light

energy, thermal methods need sufficient temperature variation and vibration based systems need sufficient vibration sources. So it is unlikely that any single method can satisfy all the energy needs for the applications. Vibration sources are generally present universally and can be readily found in the surroundings buildings, structures, etc.

Vibration energy shows a relatively high power density and among them piezoelectricity has shown the maximum power density. Vibration sources are generally more ubiquitous, and can be readily found in inaccessible locations such as air ducts and building structures [1].

As a result of devices such as Micro Electro Mechanical Systems (MEMS), portable electronics and wireless sensors, energy harvesting has become a very crucial topic, and it has drawn attention from the scientific community. Traditional power sources of many portable electronics and wireless sensors in current technology are batteries which have many disadvantages due to limited time span, finite amount of energy, maintenance requirements, possible hazardous chemicals, and environmental effects. Moreover due to its very high mass to electrical power ratio it impedes the development of light-weight and miniature wireless devices. The wireless devices are needed to be self-powered without using a battery [1]. Renewable or sustainable power sources are therefore required to either replace or to augment the capacity of batteries to increase the lifespan and the reliability of a wireless device or to realize small volume and fully self-powered electronics and to mitigate the environmental pollution caused by inappropriate disposal and recycling of batteries [2].

With the help of piezoelectric materials, various devices can be used for scavenging as well as for the diagnostics of the components of machines. Graphene has been established as an all-round solar and storage material. In this work, both the properties of the piezoelectric materials and solution are coupled together for the purpose of energy harvesting which is otherwise lost as

vibrational energy and photovoltaic energy. In subsequent sections, a review of energy harvesting with various materials using different techniques is presented.

1.3 Piezoelectricity

Piezoelectricity is the property of a material in which if a mechanical stress or pressure is applied to the material then the material generates charges as a response to the stimulus of mechanical stress. Piezoelectricity was discovered in 1880 by French physicists Curie brothers, Jacques and Pierre [3]. They demonstrated this phenomenon using crystals of tourmaline, quartz, topaz, cane sugar, and Rochelle salt. The word piezoelectric legitimately means electricity resulting from pressure. The name 'piezo' originates from the Greek word 'piezo' or 'piezein', which means to squeeze or press and 'electron' or 'electric' which actually means amber and further translates to an ancient source of electric charge. Piezoelectric effect is a reversible effect where the crystals produce electricity when they are deformed due to mechanical stress (direct effect) and conversely they will change in dimension when they are exposed to an electric field (converse effect). The converse effect was mathematically deduced from fundamental thermodynamic principles by Gabriel Lippmann in 1881. As of today it is known that many crystals, certain ceramics and even biological matter such as DNA possess the piezoelectric effect.

In the usual unstressed state the domains of piezoelectric crystals have both positive and negative charges that are symmetrically arranged within the crystal to nullify any electrical charge in the crystal. As soon as the crystal is under any kind of stress that leads to its deformation, the electron neutrality of the crystal is disturbed i.e. the charges now no longer nullify each other and it gets polarized by net positive and negative charges which appear on opposite crystal faces as shown in Figure 1.1. In stage 1 the ions are arranged in a relaxed state, stage 2 represents the balance of charges, stage 3 is during the application of stress using a finger and stage 4 shows the

arrangement of electrons with positive and negative on opposite surfaces. Figure 1.2 shows the converse piezoelectric effect.

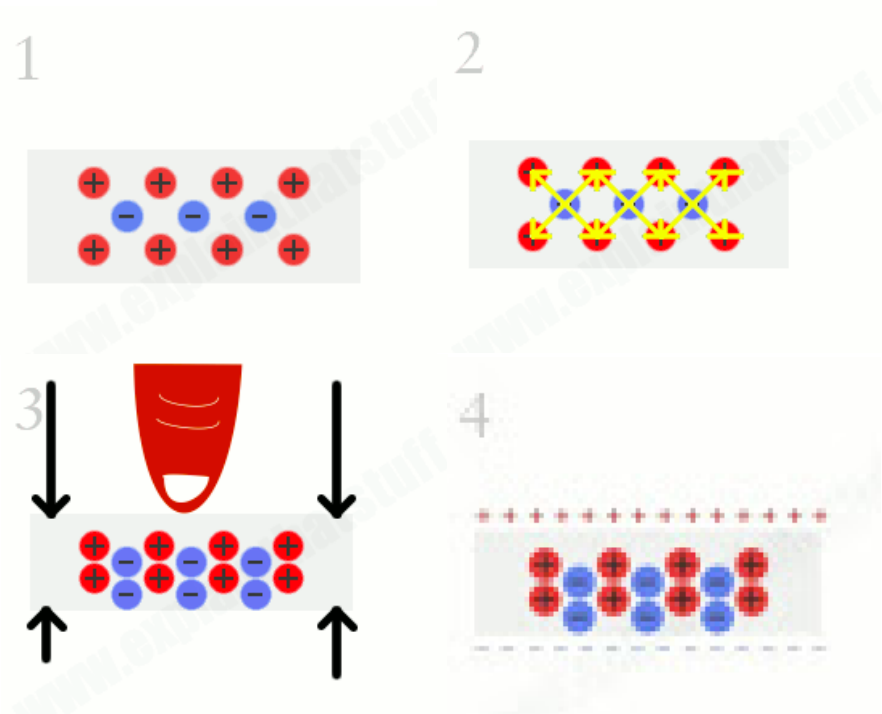

Figure 1.1 Piezoelectric concept [4]

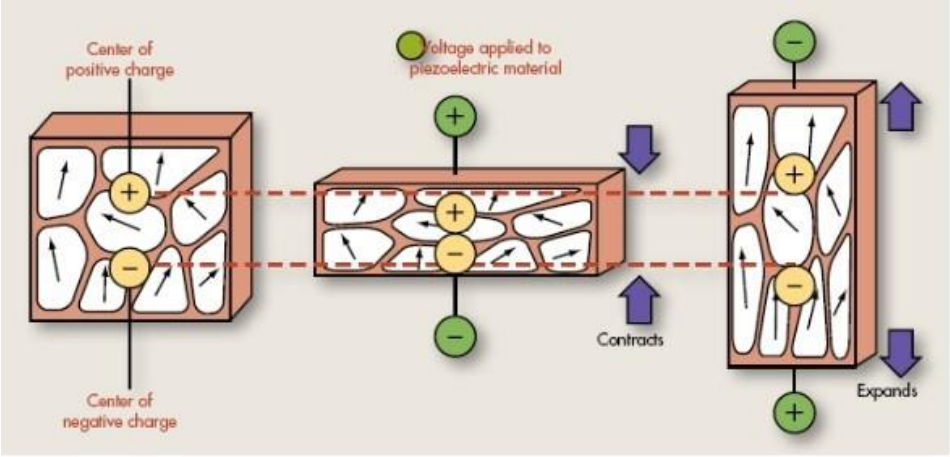

Figure 1.2 Converse piezoelectric effect [3]

In most crystals (such as metals), the unit cell (the basic repeating unit) is symmetrical; in piezoelectric crystals, it isn't. Normally, piezoelectric crystals are electrically neutral: the atoms inside them may not be symmetrically arranged, but their electrical charges are perfectly balanced: a positive charge in one place cancels out a negative charge nearby. However, if the piezoelectric crystal is squeezed or stretched, by deforming the structure, pushing some of the atoms closer together or further apart, upsetting the balance of positive and negative, and causing net electrical charges to appear. This effect carries through the whole structure so net positive and negative charges appear on opposite, outer faces of the crystal.

The reverse-piezoelectric effect acts completely in a converse way. If a voltage is applied across a piezoelectric crystal and subjected to "electrical pressure" to the atoms inside, they have to move to rebalance themselves and that is what causes piezoelectric crystals to deform (slightly change shape) when you put a voltage across them.

There are all kinds of situations where mechanical energy (pressure or movement of some kind) can be converted into electrical signals or vice-versa. Often this can be done with a piezoelectric transducer. A transducer is simply a device that converts one form of energy to another (for example, converting light, sound, or mechanical pressure into electrical signals).

Piezoelectricity is also used, much more crudely, in spark lighters for gas stoves and barbecues. Press a lighter switch and you'll hear a clicking sound and see sparks appear. What you're doing, when you press the switch, is squeezing a piezoelectric crystal, generating a voltage, and making a spark fly across a small gap.

Piezoelectric materials are widely available in many forms including single crystal (e.g. Quartz), piezo-ceramic (e.g. Lead zirconium titanate or PZT), thin film (e.g. Sputtered zinc oxide),

screen printable thick films based upon piezo-ceramic powders and polymeric materials such as Polyvinylidene fluoride (PVDF) [5-7].

1.3.1 Piezoelectric Constants and related terminologies

Three axis are used to identify directions in a piezo-ceramic element. These axes, termed 1, 2, and 3, are analogous to X, Y, and Z of a classical three dimensional orthogonal set of axes as shown in Figure 1.3. Piezoelectric coefficients with double subscripts link electrical and mechanical quantities. The first subscript gives the direction of the electric field associated with the voltage applied, or the charge produced. The second subscript gives the direction of the mechanical stress or strain. For instance in a piezoelectric constant Xij, i corresponds to the direction of the electrical value measurement, and j corresponds to the direction of mechanical action.

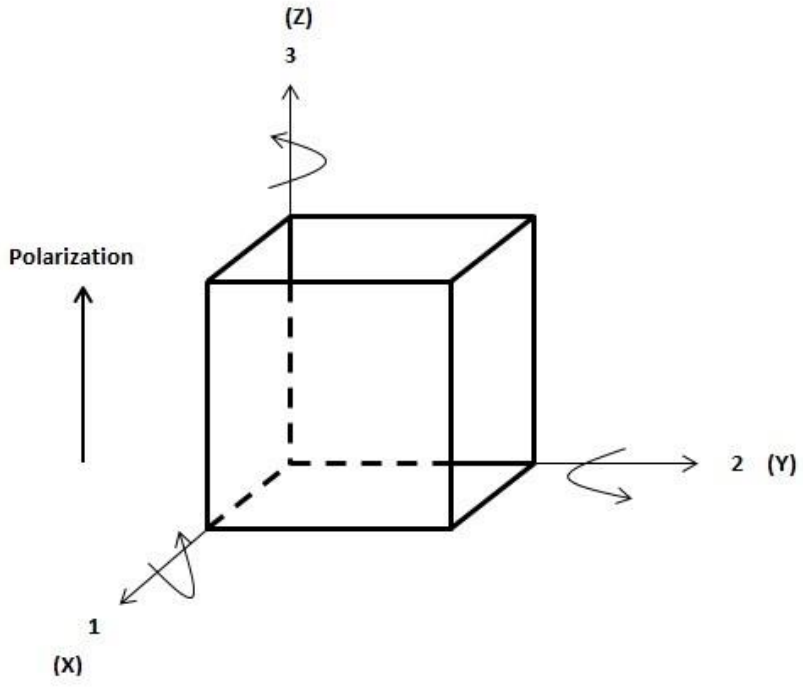

Figure 1.3 Designation of axes in piezoelectric material

According to this, a ‘31 index will characterize an electrical value considered between two sides of the film, and a mechanical stress applied along the length. In most cases, i = 3 because the electrodes are on the planar surface of the sample. Figure 1.4 shows the piezo electric coupling modes.

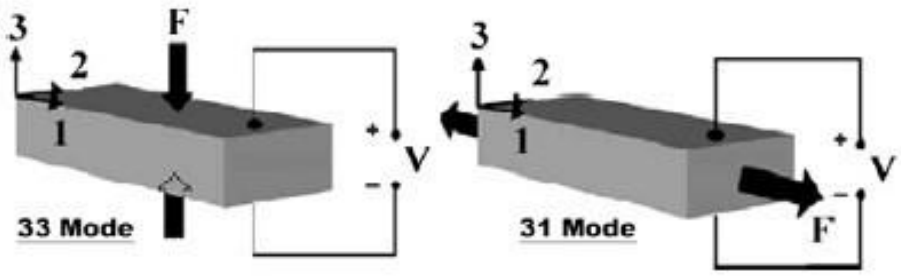

Figure 1.4 Piezo electric coupling modes [8]

The following paragraphs contain commonly used piezo terminology to describe properties of piezo material.

- ***Piezoelectric charge constant***

The piezoelectric constants or ‘d’ coefficients are relating the mechanical strain produced by an applied electric field. The units may then be expressed as meters per meter, per volts per meter (meters per volt). Conversely, the coefficient may be viewed as relating the charge collected on the electrodes, to the applied mechanical stress (coulombs per newton). d_{31} is the induced polarization in direction 3 per unit stress applied in direction 1. Alternatively, it is the mechanical strain induced in the material in direction 1 per unit electric field applied in direction 3.

- ***Piezoelectric voltage constant***

Piezoelectric voltage constant or ‘g’ constants relates the electric field produced in a material by a mechanical stress applied to it. The units may then be expressed as volts/meter per

newton/square meter. Conversely, it is the mechanical strain experienced by the material per unit electric displacement applied to it. g_{31} is the induced electric field in direction 3 per unit stress applied in direction 1. Alternatively, it is the mechanical strain induced in the material in direction 1 per unit electric displacement applied in direction 3.

- ***Coupling factor***

Electromechanical coupling factor 'k' is a measure of conversion of energy by the piezo element from electrical to mechanical form or vice versa

$$k = {}^{p}(\text{Mechanical energy stored / Electrical energy applied}) \quad (1.1)$$

or

$$k = {}^{p}(\text{Electrical energy stored / Mechanical energy applied}) \quad (1.2)$$

Coupling factor carries subscripts, for instance k_{31} relates to a long thin bar, electrode on a pair of long faces, polarized in thickness, and vibrating in simple length expansion and contraction.

- ***Compliance***

Compliance S of a material is strain produced per a unit stress. The first subscript refers to the direction of strain and the second subscript refers to direction of stress. For instance S_{11}^{E} is the compliance for a stress and accompanying stain in direction 1 under conditions of constant electric field.

- ***Permittivity***

Permittivity or dielectric displacement *is* measure of the ability of a material to resist the formation of an electric field within it. Permittivity is expressed as the ratio of its electric

displacement to the applied field strength and measured in farads per meter. The permittivity of a medium is most often given as a relative permittivity

$$\epsilon_r = \epsilon/\epsilon_o.$$

- ***Capacitance***

Capacitance is the ability of a body to store an electrical charge. Capacitance is a function of the physical dimensions and the permittivity.

$$C = \epsilon A/t \tag{1.3}$$

where A is the surface area and t is the thickness of the material.

1.4 Comparison of Common Piezoelectric Materials

The properties of PZT are defined in terms of constants as permittivity (ε), piezoelectric charge constant (d), piezoelectric voltage constant (g), coupling factor (k) and properties such as density and acoustic impedance. Table 1.1 [9] demonstrates the superior properties of PZT as compared to other piezoelectric materials.

Table 1.1 Properties of different piezoelectric materials [9]

Property	**Symbol**	**Units**	**PVDF Film**	**PZT**	**$BaTiO_3$**
Density	ρ	10^3 kg/m3	1.78	7.5	5.7
Relative Permittivity	ϵ/ϵ_o	ε/ε0	12	1200	1700
Piezo electric Charge Constant	d_{31}	(10^{-12}) C/N	23	110	78
Piezo electric Voltage Constant	g_{31}	(10^{-3}) Vm/N	216	10	5
Coupling Factor	k_{31}	% at 1 KHz	12	30	21
Acoustic Impedance		(10^6) kg/m^2-sec	2.7	30	30

Piezoelectric materials are smart materials used in MEMS. They possess a unique property called piezoelectricity, which if mechanically stressed generates a potential difference given in

voltage. Piezoelectric materials are naturally available and are also in the form of multiphase ceramics and films. Some of the man-made piezoelectric ceramics are barium titanate, lead titanate, lead zirconium titanate (PZT), and lithium niobate.

1.5 Lead Zirconate Titanate (PZT)

Lead zirconate titanate ($Pb[Zr_xTi_{1-x}]O_3$, where $0<x<1$) or PZT is an intermetallic inorganic compound that shows different crystal structure at different temperatures [10-12]. It has perovskite structure below Curie temperature (which ranges from 510 K to 800 K) and above Curie temperature it has paraelectric cubic structure. Also, below Curie temperature the cubic perovskite structure is distorted to a rhombohedral structure or a tetragonal structure for rich Ti based PZT. Its structure consists of oxygen and small Ti or Zr atoms in symmetrical octahedral sites, with Pb cations occupying dodecahedral sites, as shown in Figure 1.5. The atomic size of lead and oxygen are 1.4 Å each. Lead, oxygen, and titanium/zirconium atoms together form a face centered cubic array.

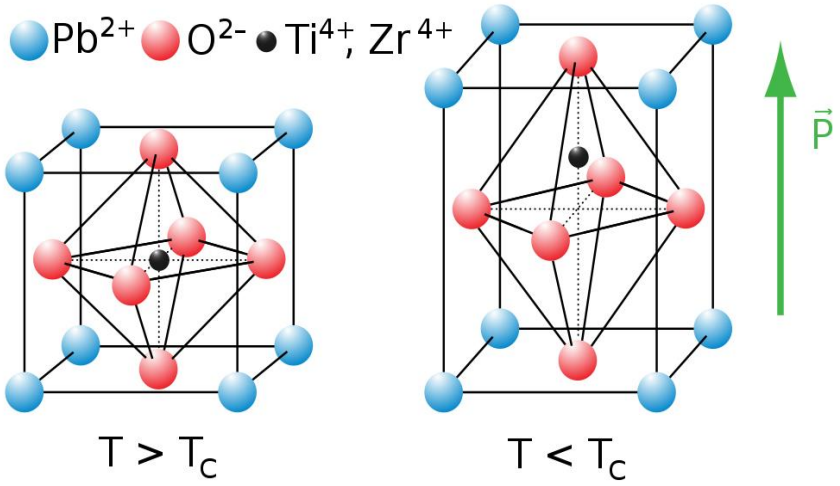

Figure 1.5 Left is structure of PZT and right under influence of an electric field [13]

The Curie temperature (T_c) is a transition temperature of ferroelectricity and is defined as $\varepsilon = C/(T-T_\theta)$, where ε is the permittivity, C is the Curie constant, and T_θ is the Curie-Wiess

temperature. As the composition of Zr or Ti, the PZT has a different phase between the rhombohedral and tetragonal. The boundary of those two phases is called the morphotropic phase boundary (MPB) around Zr/Ti composition of 0.52/0.48. The tetragonal structure has six <100> polarization directions and the rhombohedral structure has eight <111> polarization directions. The maximum piezoelectric and dielectric constants are commonly observed at MPB due to high probability of 18 polarization, and they are more sensitive to the composition than to the temperature because the MPB is very vertical. The phases of PZT have been plotted in Figure 1.6.

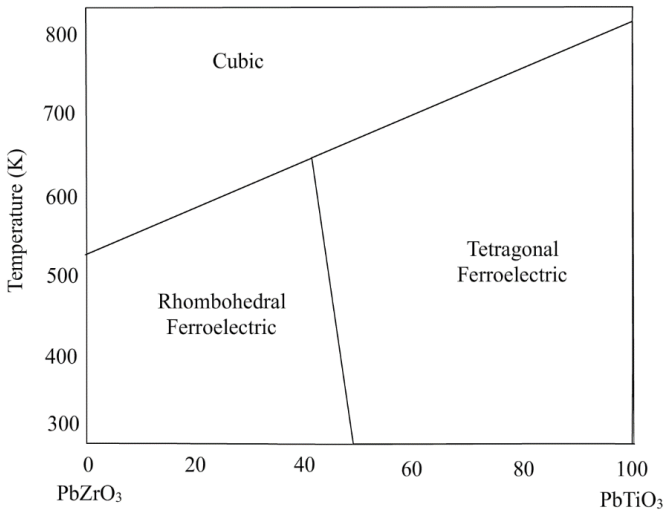

Figure 1.6 Phase diagram of PZT at different temperature with increasing amount of Ti and decreasing amount of Zr [14]

Although all piezoelectric materials work on the same principle, PZT has highly advanced features and properties. PZT has a wide operating frequency range from 10^{-3} Hz to 10^{9} Hz. Also, it has low acoustic impedance, high elastic compliance, high stability, mechanical strength and resistivity against moisture and chemicals with its only shortcoming being a brittle material, making it very suitable for energy harvesting and thus was chosen over the other piezo materials for this work.

1.6 Vibration Based Energy Harvesting from piezoelectric materials

While there are four main methods of energy harvesting (vibration, thermal, photovoltaic, electromagnetic), the current work revolves around the vibration based energy harvesting and methods to improve it. Mechanical vibration is one of the most effective methods of implementing a power harvesting system. Mechanical vibration when applied to a piezo film causes strain in the film and thus converting the strain energy into electrical energy. There are many methods of collecting and storing the produced charges like capacitor charging, battery charging, etc. Research in the field of vibration based energy harvesting have made various electronics systems (ranging from digital electronics to wireless transmitters) self-powering [15-18].

Piezoelectric materials exhibit anisotropic characteristics, thus the properties of the material differ depending upon the direction of forces and orientation of the polarization and electrodes. The anisotropic piezoelectric properties of the ceramic are defined by a system of symbols and notation. Piezoelectric materials can be generalized for two cases. When the PZT are kept in stack configuration that rely on a compressive strain applied perpendicular to exploit the d_{33} coefficient of the material whereas those that apply strain parallel to the electrodes utilize the d_{31} coefficient [22-23]. The concept for implementing piezoelectric materials with graphene is to provide a sustainable power source is attracting a lot of scientific community attention [24].

1.7 Nanogenerators (NG)

There have been several different types of piezoelectric materials that has been used as nanogenerators like semiconducting piezoelectrics, insulating piezoelectrics and insulating polymeric piezoelectrics.

1.7.1 Semiconducting Piezoelectric Materials:

ZnO is a semiconducting piezoelectric material, nanogenerators has its ZnO nanostructures like nanoparticles, nanowires, nanorods, nanobelts, nanotubes, nanopowder and other complex forms [25-26]. Wang and Song took the first step in the development of NGs using the piezoelectricity of aligned ZnO nanowires (NWs) with the help of atomic force microscopy (AFM) [27] as shown in figure 1.7.

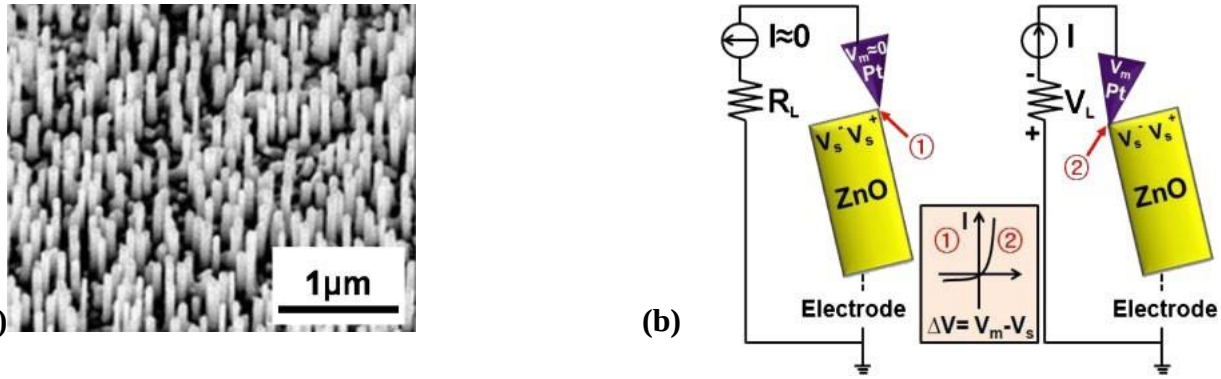

Figure 1.7(a) Reproduced SEM image of vertically aligned ZnO NWs by Wang and Song [27] (b) Schematic representation of measurement of output voltage due to the bending of ZnO NW during the scanning of AFM tip over NWs [27]

1.7.2 Insulating Piezoelectric Materials:

BaTiO3, PVDF and PZT; Researchers were not limited to ZnO, they have discovered their luck with insulating piezoelectric materials like BaTiO3 and PZT. Due to its excellent piezoelectric properties (d_{33} = ¼ 60{130 pC/N) over those of ZnO (d_{33} = ¼ 5:9 pC/N) and other materials, PZT acted as the most promising perovskite material. Its output has a significant advantage over other semiconducting piezoelectric materials. With different PZT composition ratio's, $Pb(Zr_{0:52}Ti_{0:48})O_3$ near the morphotropic phase boundary (MPB) exhibits excellent ferroelectric and piezoelectric properties, which qualifies as the most suitable NG. To achieve the piezoelectric properties of these insulating materials they are heated to Curie temperature. To rearrange the ions in the poling axis a sufficient voltage is applied in the desired direction. The orientation of ions in the poling

direction is maintained even when they attain lower temperature. The amassing of unlike charges at the two ends of the material's surfaces is due to external strain on the charge center of dipoles following the poling process [28].

Schematic example of PZT nanofiber-based NGs device in which interdigitated electrodes are connected to the extraction electrodes for harvesting the charge carriers and a soft polymer PDMS is attached on top of PZT fibers to package the device [28]

Another subset of insulating piezoelectric materials is the piezo-polymer material. Its most researched piezoelectric polymer is PVDF which has good flexibility, lightweight and biocompatibility. However, it has relatively low piezoelectric coefficient (25pC/N) because of the limitation of the alignment of the H–C–F dipoles and randomly oriented crystals. The comparison table of various NG's and their parameters have been listed in Table 1.2.

Table 1.2 Comparison of various parameters of NGs such as: type of material, shape and size, active area, piezoelectric coefficient (d_{33}), output voltage (V_{out}), output current (I_{out}), current density (J_{out}), and power density (P). [29]

Material	Structure	Substrate	Dimension	Electrode	d33 (pm/V)	Output voltage	Output current/current density	Power/ Power Density	Ref.
ZnO	Lateral nanowires	Flexible substrate	D: 200nm L: 50 μm A: 1cm^2	Au	14.3–26.7	2.03V	107nA	11mW/cm^3	[30]
ZnO	Array of nanowires	PDMS	D: 500nm L: 6 μm A: 1.5cm^2	ITO	14.3–26.7	8V	0.6A	5:3mW/cm^3	[31]
PVDF	Nanofibers	Grounded substrate	D: 0.5–6.5 μm L: 0.1–0.6mm A: /	Metal	57:6	5–30mV	0.5–3nA	2.5–90pW per cycle (calculated)	[32]
PZT	Ribbon film	PET film	Ribbon size:500 μmx100 μm T: 500nm A: 60mm^2	Graphene	250	2V	2:2mA/cm^2	88mW/cm^3	[33]
PZT	Nanowires	PET film	L: 1.5cm W: 0.8mm T: 5 μm A: /	Ag	152	6V	45nA	200W/cm^3	[34]
$BaTiO_3$	Ribbon film	Kapton film	Ribbon size:300 μmx50 μm T: 300nm A: 82mm^2	Au	30–100	1V	0.19A/cm^2	7mW/cm^3	[35]

1.8 Zinc Oxide Nanoparticles

Zinc oxide is an inorganic compound with the chemical formula ZnO. Its molecules have tetrahedral structure. The bonding in ZnO is largely ionic, which explains its strong piezoelectricity. Zinc oxide possess both the semiconducting and piezoelectric properties which makes it unique. It is bio-safe and biocompatible material which makes increases its stakes on sustainability. ZnO has the highest piezoelectric tensor among other tetrahedrally bonded semiconductors like ZnO, GaN, CdS and ZnS. In all these materials, the piezoelectric effect is the result of two different terms of opposite signs. These terms are usually referred to as the clamped ion and internal strain contributions. ZnO has the least cancellation effect among them which accounts for its high piezoelectric effect [36-37].

ZnO has a non-central symmetric wurtzite crystal structure. Zn^{2+} cations and O^{2-} anions are placed in tetrahedral coordinates and the centers of the positive and negative ions overlap. If a stress is applied at an apex of the tetrahedron, the centers of the cations and anions are relatively displaced, resulting in a dipole moment. Figure 1.8 shows this effect. Polarization from all of the units results in a macroscopic potential (piezopotential) drop along the straining direction in the crystal [38]

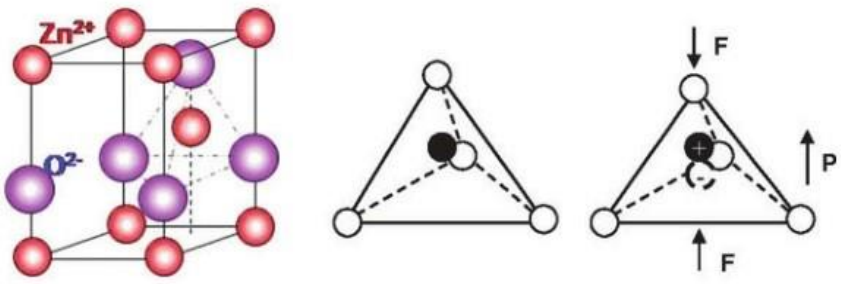

Figure 1.8 ZnO crystal structure [38]

ZnO is a promising material for the future of nanotechnology. ZnO has wide energy gap (3.37 eV), high excitation binding energy and high breakdown strength which makes it highly suitable for the electronic and photonic devices as well as for high frequency applications. Availability of ZnO in native substrate form and its potential for room temperature operations makes ZnO highly desirable for chemical sensors and subscale operations. ZnO has higher excitation binding energy (60meV) compared to other semiconductor materials. Because of having higher band energy, ZnO is useful in the field of piezoelectricity, ferroelectricity and ferromagnetism [39].

1.9 Ferro Fluid Nanoparticles

Ferrofluids are colloidal mixtures composed of nanoscale ferromagnetic or ferrimagnectic particles. These particles are suspended in a carrier fluid usually an organic solvent or water. The ferromagnetic nanoparticles are coated with a surfactant to prevent their agglomeration due to van der Waals forces and magnetic forces. Oleic acid, citric acid, tetra methyl ammonium hydroxides are the common surfactants used. Nano-size ferrofluid particles are suspended by Brownian motion and hence they generally do not settle under normal conditions [40].

Ferrofluids have an important property of changing their physical properties by means of moderate magnetic fields, especially their viscosity. This property makes ferrofluid very useful in the fields of engineering and medicine. This property of ferrofluid is known as the magneto viscous effect [41]. They have a strong affinity towards magnets, they are basically paramagnetic materials and as soon as they are exposed to magnets they become strongly magnetized as shown in Figure 1.9

Figure 1.9 Ferrofluid under effect of magnetic field [42]

The composition of the constituents in the ferrofluid used is 5% magnetic particles which is iron, 15% Surfactant i.e. oleic acid or polymers and 80% carrier fluid i.e. mineral oil like kerosene or water. A typical ferrofluid is illustrated in Figure 1.10.

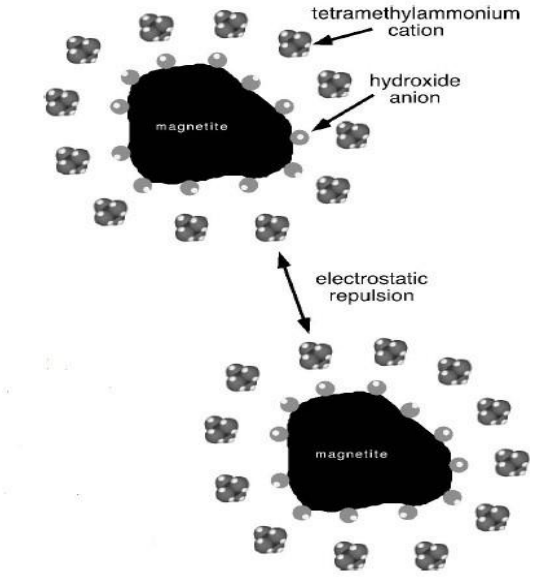

Figure 1.10 Ferrofluid constituents [42]

In this figure the Tetramethylammonium hydroxide coats the magnetite particles with hydroxide anions. Tetramethylammonium hydroxide cations create diffuse shell around each magnetite particle and create repulsion between particles stabilizing the colloid. [42].

The magnetic moment of the ferrofluid particles are randomly distributed. Thus they have no net magnetization. Under the influence of a magnetic fluid, the magnetic moments of the particles orient along the fields lines forming cones. Under the magnetic field, ferrofluid responds as a homogenous magnetic liquid moving to the region of highest flux. Retention force of a ferrofluid can be adjusted by either changing the magnetization of the fluid of the magnetic field in the region [40].

1.9.1 Formation of cones

When ferrofluid is subjected to a magnetic field they act as magnets due to their paramagnetic behavior. Since the constituent of ferrofluid is magnetic nanoparticles, when exposed to a magnetic field they tend to form a trajectory towards the magnetic lines of forces, which leads to the formation of circular based structures with a pointed head resembling a conical structure. The size of these cones can be varied by the variation of magnetic field, also if they are exposed to this field for a long time under some source of heat or in atmosphere which dries out the carrier fluid. When the magnetic field is removed, after a sufficient amount of time for the carrier fluid to dry out, iron oxides nanoparticles in the form of cones are left. Since these ferrofluid have does not a strong binding force an external binder like epoxy is required to hold the structure and resists external vibrating forces to let them fell off.

1.10 Graphene

This is the era of graphene, it's the rising star on the grounds of materials science and condensed matter physics. It's strictly a two-dimensional material and it is a one atom thick allotrope of carbon having a honeycomb structure. It inherits significantly high crystal and electronic quality and, despite its short history, has already revealed a profusion of new physics

and potential applications, which are briefly discussed here. It's a zero-gap semiconductor [43] and its single layered structure has helped to access its peculiar electronic properties. Whereas one can be certain of the authenticity of applications only when commercial products appear, graphene does not require any credibility of its prominence in terms of fundamental physics. Owing to its unusual electronic spectrum, graphene has led to the emergence of a new archetype of "relativistic" condensed matter physics, where quantum relativistic phenomena, some of which are unobservable in high energy physics, can now be simulated and examined in table-top experiments. More generally, graphene represents a conceptually new class of materials that are only one atom thick and, on this basis, offers new inroads into low-dimensional physics that has never ceased to surprise and continues to provide a fertile ground for applications [44]. It has shown very optimistic results when used as a storage device as an ultracapacitor [45].

Graphene is basically non-piezoelectric but can be persuaded to act like a material to produce electricity under mechanical stress by creating holes of the right symmetry and can acquire a piezoelectric coefficient almost 36% of Boron nitrite nanotubes and 72% of that of quartz [46]. It shows excellent photovoltaic material properties and recently researchers have synthesized solar dies based on graphene [47-49]

1.11 Improving Efficiency of Energy Harvesting using Nanoparticles Coating

Researchers have investigated the efficiency of the piezoelectric stack operated in compression and found that efficiency does increase with increasing force and load resistance but these factors are less significant than frequency as efficiency was found maximum at several orders of magnitude below the resonant frequency [50]. A low cost, approach to produce electricity using piezoelectric zinc oxide nanowires gifted of converting low-frequency vibration/friction energy into electrical energy [51].

It is found that PZT thick films fabricated through screen printing show porosity ranging from 10% to 40% [52]. Researchers have studied the results by varying the thickness and length of piezoelectric materials [53]. This high percentage of PZT greatly affects the electromechanical properties resulting in a decrease in the amount of energy harvested from them. Basic properties of PZT, like the ferroelectric, electromechanical coupling, hysteresis and dielectric constant have a great role in determining the wide range applications of PZT. Researchers are trying to improve these properties by doping, surface treatment and coating. Studies have been conducted to explain the effect of complex doping on the structure and electrical properties of PZT ceramics. The properties of the PZT ceramics modified with complex soft dopants, La^{3+} and Nb^{3+} with non-modified PZT and the modified PZT ceramics showed enhanced piezoelectric properties and were stable with the compositional variations [54]. Local crystallographic orientation and the local grain-grain orientation affect the ferroelectric properties of the PZT. These properties play an important role in determining switching of domains. Piezo force microscopy was an important tool used for analyzing the polarization switching behavior at the grain corners and boundaries [55]. In this work, zinc oxide nanoparticles along with ferrous ferro-fluid nanoparticles and graphene are used to improve the efficiency of energy harvested from vibration of PZT and luminance effect have been studied. The properties of all nanoparticles are listed in Table 1.3 below.

Table 1.3 Properties of Nanoparticles

Properties	ZnO nanopowder	Ferrofluid	Graphene
Size of Nanoparticles (nm)	01 - 10		25
Appearance	White	Black	Black
Physical form	Powder	Solution	nanoplatelets
Density(g/cc)	5.643	1.21	2.2
Young Modulus (Gpa)	12		1000
Poissons ratio	0.31		
Specific Heat @ 25°C ($Jmol^{-1}K^{-1)}$	0.12		
Thermal Conductivity(watts/meter-K)	251		3000
Electrical conductivity (siemens/meter)			10^7
Magnetic Ordering	Diamagnetic	Paramagnetic	Diamagnetic
Band Gap (eV)	3.3		0
Excitation Binding Energy (meV)	60		
Piezo Electric effect (F/m^2)	1.2		
Electron Mobility $cm^2/(V \cdot s)$ @ 80 K	27		200,000
Viscosity (cp@27°C)		6	
Acoustic Impedance (g/cm^2-sec)	$36.4x10^5$		

ZnO hybridized with graphene can produce an efficient photocatalyst [19-21]. Veeregowda [56] at the University of Mississippi, verified this by testing them under various experiments that ferrous nanoparticle coated from ferrofluid on silver coated PZT material of area 6 in^2 can enrich the energy generation. His experiment reveals a boost from 51.123 mV to 115.434 mV comparing a plain PZT with the coated PZT vibrating at a frequency of 90Hz.

Bhagmar [57] and Sharma [58] in their work at the University of Mississippi showed a rise in the output from 237 mV to 299.7 mV and 48.5 µW to 68.5 µW (by applying a magnetic field of 160 gauss) when coated with FNP-ZnO coat. The data above shows that the nanoparticle coating has good potential for power generation.

1.12 Justification of work

From the above literature search it is apparent that to enhance the power output of smart piezoelectric materials, nanoparticles and magnetic effect in combination can be used. Hence this current research is thus focused on development of a smart composite with various combinations of coatings of nanoparticles of FNP and ZnO, graphene, under the influence of magnetic field and luminance under various frequencies.

This research involves developing a coating which is easier to make and apply on PZT. The coating developed was formed using readily available materials like graphene, FNP, ZnO nanoparticles, and commercially available magnetic strips and binder resins. The cost involved in developing this coating is economical and low as compared to other materials having different composites used for energy harvesting.

The major advantage(s) of using this coating was that it utilizes Opto-MagnetoElectric effect, which is a combination of the optical effect of graphene and ZnO nanoparticles and advanced magenetoelectric effect of both FNP and ZnO. These properties should enhance the power density of the coating and provides an easier and cost effective alternative for improving the energy harvesting capabilities and versatility of PZT at various environments.

In addition to this the other focus was on making PZT-composite based solar cells to tap and store solar energy. Also, the combination of solar cells and piezoelectric materials can be used to create a composite which has the potential to use both vibration and solar energy simultaneously.

CHAPTER 2. EXPERIMENTAL DETAILS

2.1 Preparation of nano-paste coating solution:

Sudhanshu [58] found in his work at the University of Mississippi that the maximum output of power using the mixture of ferrofluid nanoparticles, zinc oxide nanoparticles and epoxy was achieved with 59.9% ferrofluid, 40% ZnO and 0.1% epoxy. This process was progressed with the addition of graphene and the effect of light on the substrate was studied. For the first set of experiments for energy harvesting, two sets of composites were compared, one was PZT mounted on a rectangular plate and the other was nano-coated PZT with different constituents of different composition. The process is explained in the Figure 2.1 below.

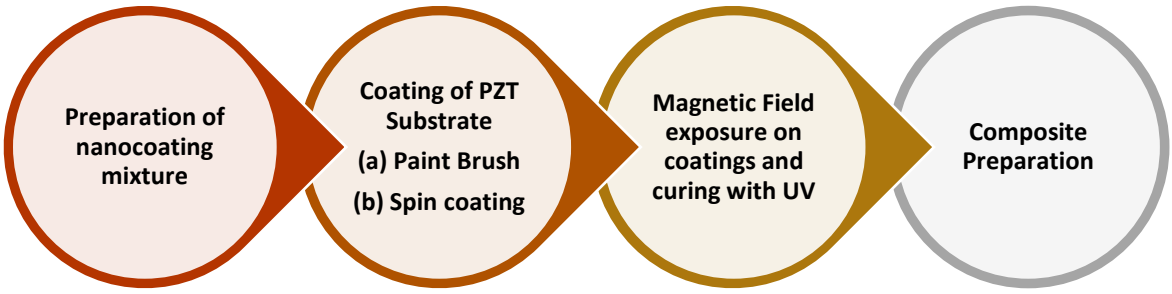

Figure 2.1 Flowchart of steps involved in composite preparation

2.1.1 Optimization of Epoxy used in solution

A total of 4 different nano-coating mixtures were produced with different ratios of constituents to optimize the amount of epoxy keeping zinc oxide nanoparticles content constant and varying the amount of ferrofluid nanoparticles. Details of the solutions prepared is shown in Table 2.1

Table 2.1 Different compositions of composite coatings for optimization of epoxy

S. No.	Ferrofluid %	ZnO %	Epoxy %	Graphene %
1	59.9	40	0.1	0
2	59.5	40	0.5	0
3	59	40	1	0
4	58	40	2	0

Epoxy acts as a binder in this solution, but it absorbs the vibrations in the sample which can decrease the energy output. Optimum amount of epoxy was determined to maintain the balance of holding the solution together and has minimum effect on vibrations in the specimen.

First step was the preparation of epoxy in a mixing bowl, epoxy has 2 constituents A and B that were in different bottles, and they were added in the ratio of 10:1 by weight. For preparation of 1 gm of epoxy the amount of A and B added was 910 mg and 9 mg respectively. 10 gm of each solution was prepared, so for every 10 gm of solution 4 gm of ZnO nanopowder was used and 5.99 gm, 5.95 gm and 5.9 gm of Ferrofluid nanoparticles and 0.01 gm, 0.05 gm and 0.1 gm of epoxy was used for solution 1, 2, 3 respectively.

For the preparation of samples, the components were mixed in a centrifugal tube by weight, for instance for the preparation of solution 1, having 59.9% ferrofluid nanoparticles, 40% ZnO nanoparticles and 0.1% epoxy was used. The centrifugal tube was placed in a weighing machine

and then the weight was calibrated to zero and 4000 mg of ZnO nanoparticles was added using a spatula, and weight was calibrated to zero again and 5990 mg of Ferrofluid nanoparticles was added using a pipette and then 10 mg of Epoxy was added from the mixing bowl using a spatula in the solution. After the addition of all the constituents the centrifugal tube was shaken and when the nanopaste was prepared it was kept for sonication for 30 minutes for mixing. It avoids agglomeration of particles and make the solution consistent.

2.1.2 Optimization of constituents used in solution:

Four nano-coating mixtures were produced with different ratio of constituents to optimize the amount of constituents keeping the amount of epoxy 1% in each case and varying the amount of ferrofluid nanoparticles, zinc oxide nanopowder and graphene. For preparation of solution nmp was used since graphene [59] and ZnO [15] are soluble in it. The list of materials used is listed in Table 2.2

Table 2.2 Mixture constituents and the suppliers.

S.No	Material	Supplier and Address	Key properties
1	Ferrofluid – EMG 300	Ferrotec (USA) Corporation 33 Constitution Drive, Bedford, N.H. 03110	5%: magnetic solid (ferrofluid nanoparticles), density of FNP 5.17g/ml 10%: Surfactants 85%: carrier Density of solution= 1.21gm/ml
2	Zinc Oxide Nanopowder	Sigma-Aldrich Po box 14508 st. Louis, MO 63178 united states	Size <100 nm
3	Epoxy Resin - ITW Consumer 62345 - 437541	Ron's Home And Hardware 215 North College Avenue Indianapolis, IN 46204	-
4	Graphene-XGnP 25	XG Sciences, Inc. 3101 Grand Oak Drive, Lansing, MI 48911	Nanoplatelets, size 25 µm

For the optimization of power output with graphene in the mixture, four solutions were prepared and compared with solution 3. While preparing the solutions having graphene nanoplatelets in them, it was agglomerated together and to disperse them thoroughly in the solution, nmp (N-Methyl-2-pyrrolidone) was added in the solution and acts as a solvent for graphene. These solutions were sonicated for 2 hours so that the solution would be thorough and consistent and this would lead to a colloidal solution. The solutions prepared are tabulated in Table 2.3 below.

Table 2.3 Different compositions of composite coatings.

S. No.	Ferrofluid %	ZnO %	Epoxy %	Graphene %
5	54	40	1	5
6	49	40	1	10
7	39	40	1	20

2.2 Coating the PZT substrate surface:

The PZT substrate supplied by Murata (part number - 7BB-27-4L0) was coated with a nano-mixture by two methods, one using paint brush and the other was spin coating technique.

2.2.1 Coating PZT using paint brush technique

With the help of a paint brush the coating was distributed evenly with a uniform thickness, manually. The piezo substrate shown in the Figure 2.2 [60] with its dimensions in Table 2.4. Coating the surface of PZT substrate surface using a brush on the surface (note the amount of nano-mixture was applied in a way to avoid dripping from the sides) uniformly.

Table 2.4 Dimension of the piezo substrate [60]

Plate size dia **ø D (mm)**	Piezo element dia. **ø a (mm)**	Silver coated electrode diameter **ø b (mm)**	Total Thickness **T (mm)**	Brass Plate Thickness **t (mm)**	Plate Material
27.0	19.7	18.2	0.54	0.30	Brass

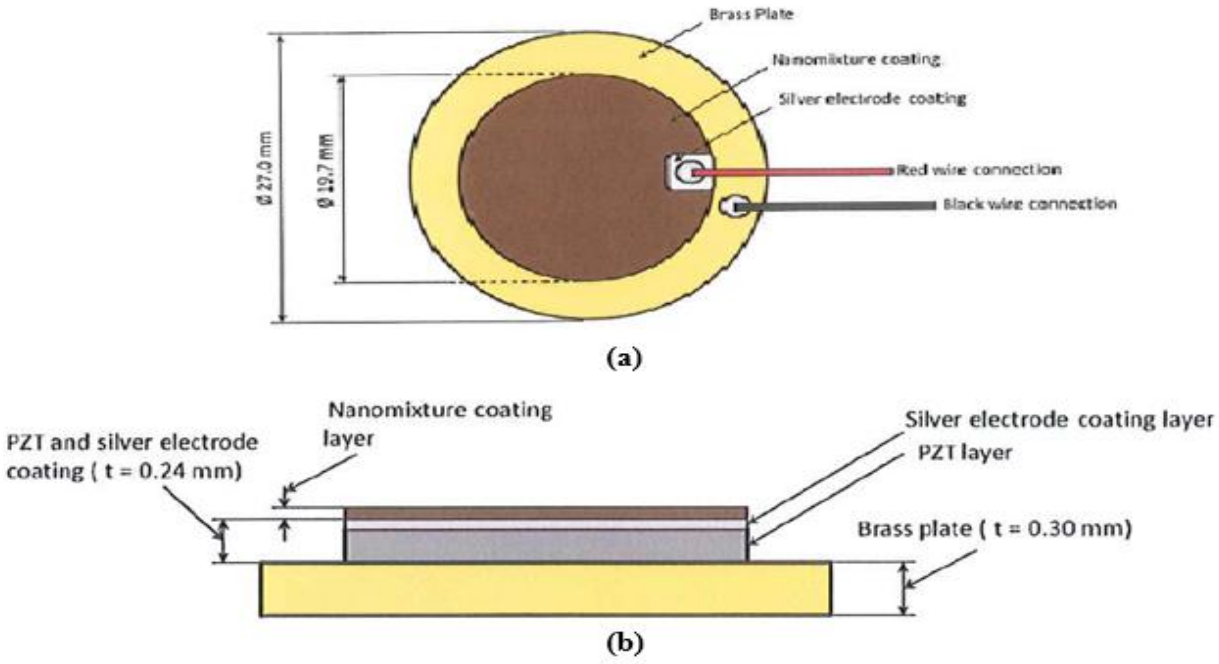

Figure 2.2 PZT substrate [60]

2.2.2 Spin coating of PZT substrate

The substrate was coated with the help of a spin coating machine located in the Chemical Engineering Department (model WS-400BZ-6NPP/LITE). The principle behind spin coating is the centripetal acceleration which causes most of the solution (resin) to spread to the edge of the substrate, leaving a thin film of material on the surface. Final coating thickness and its properties depend on the nature of the fluid material (viscosity, drying rate, percent solids, surface tension, etc.) and the parameters (speed, acceleration and time) chosen for the spin process. The spin

coating technique gives the repeatability, but with a slight change in parameters the coating film can change drastically.

Spin coating was started by constraining the boundary of the substrate, loading the substrate, switching on vacuum pump and turning the valve of nitrogen gas to 60 psi. Then a program was chosen and the solution (resin) was loaded in a pipette and then it was dropped on the center of PZT. The program was the run and at the end of run the coated PZT was obtained. The flow chart in Figure 2.3 summarizes the steps used. After steps 1-5 it was repeated by following steps 6, 7 then 4, and 5, so the order was steps 1-7 then steps 4-7 for next samples.

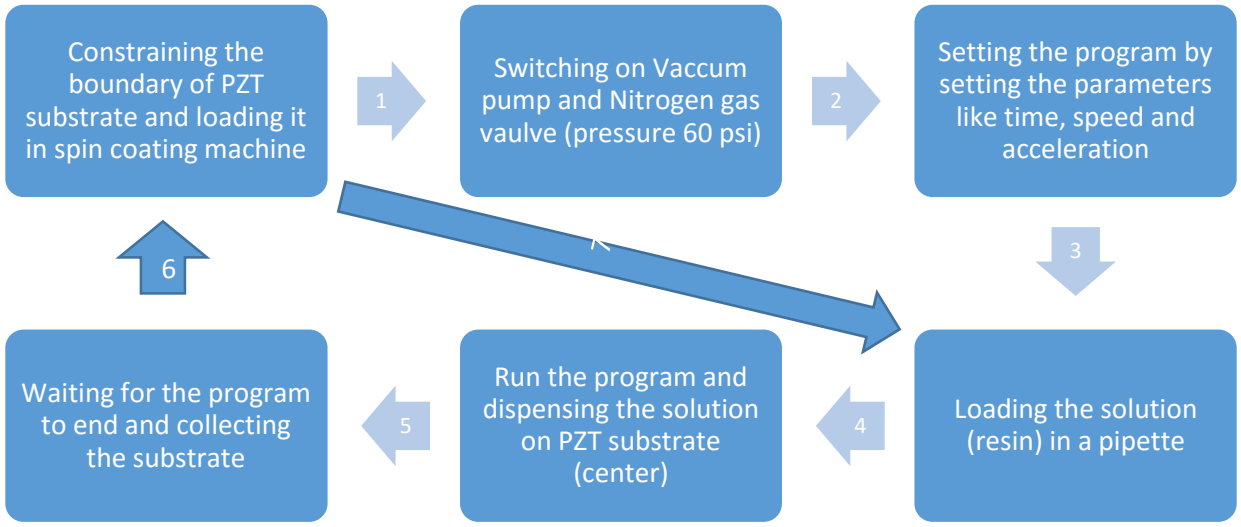

Figure 2.3 Flow chart for spin coating of PZT substrate

Approximately 0.25 ml of solution was used to coat a single substrate. The piezo substrate having a PZT layer was enclosed with a non-permeable boundary so that the coating would be restricted to PZT surface only and there is no coating over brass. Considering the low viscosity of the solution, the parameters were chosen accordingly and trials were performed to determine the best coating results came out for a coating time of 35 seconds, with a speed of 300 rpm. The actual setup is shown in Figure 2.4

Figure 2.4 Actual setup of spin coating

2.3 Curing with UV Rays and exposure to magnetic field:

The nanocoated PZT substrate was then exposed to a magnetic field with magnets on top and bottom kept at a certain distance and exposed to ultraviolet light (UV) for curing. The combination of magnetic field and distance between the magnets should be optimized to 12" and 160 Gauss for the cones on PZT surface to be of highest height with maximum density and it should not fell of as soon as the magnetic force is removed. The UV curing process is based on a photochemical reaction. A UV lamp (Entela UVL-56) having a wavelength 365 nm was used for curing. The curing time was 24-30 hours for all the test specimens, so they are dried and firm. The chamber used for curing is shown in Figure 2.5.

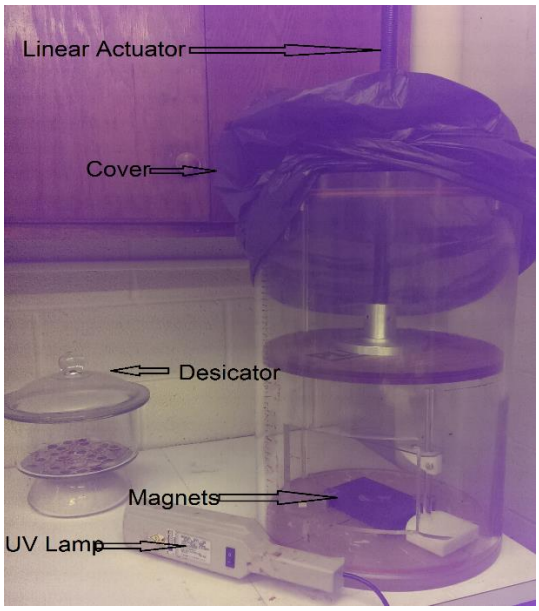

Figure 2.5 Chamber used for magnetic exposure and curing

A schematic diagram of the exciter and placement of substrates on the plates is shown in Figure 2.6. The substrates was connected in series and were placed at a distance of 60 mm from the fixed end. The distance between the substrates were maintained at 29mm from their respective centers. The thickness of steel plate was 0.5 mm.

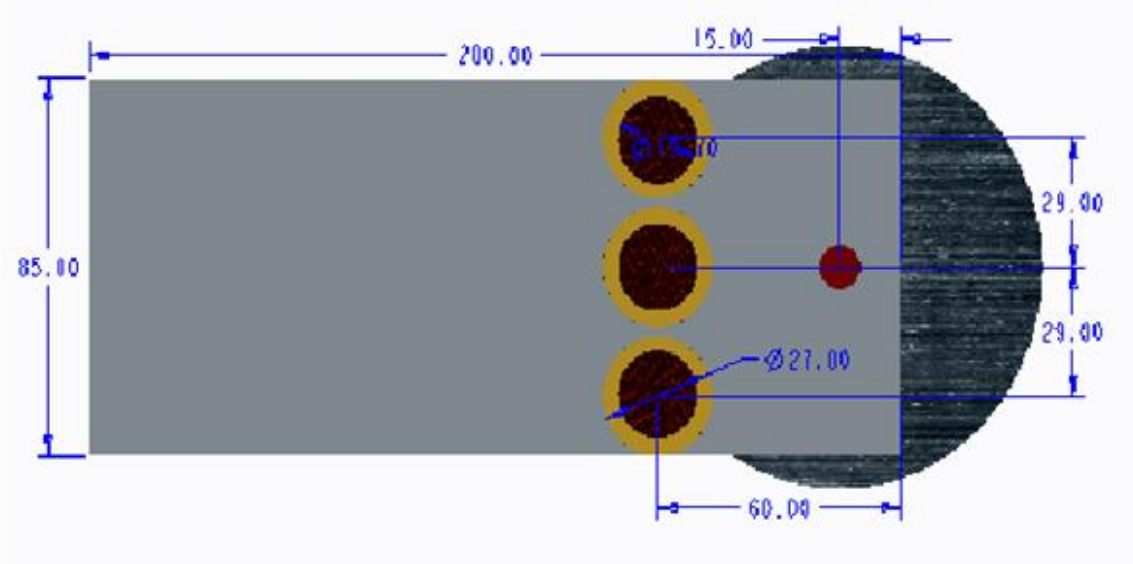

Figure 2.6 Exciter, rectangular plate and Piezo positions, all dimensions are in mm

The setup of the experiment is shown in Figure 2.7 which includes a signal generator for establishing an output which is enhanced using an amplifier. This is further connected to a vibrator or exciter that vibrates at various frequencies as programmed by the signal generator and the output of the voltage root mean square value can be seen using oscilloscope. This V_{rms} value can be used to calculate the power output for each frequency. The power per second was calculated by summing up the area under the curve of power and frequency. A frequency range from 65 Hz to 400 Hz was used for the calculation of net power produced in that frequency range.

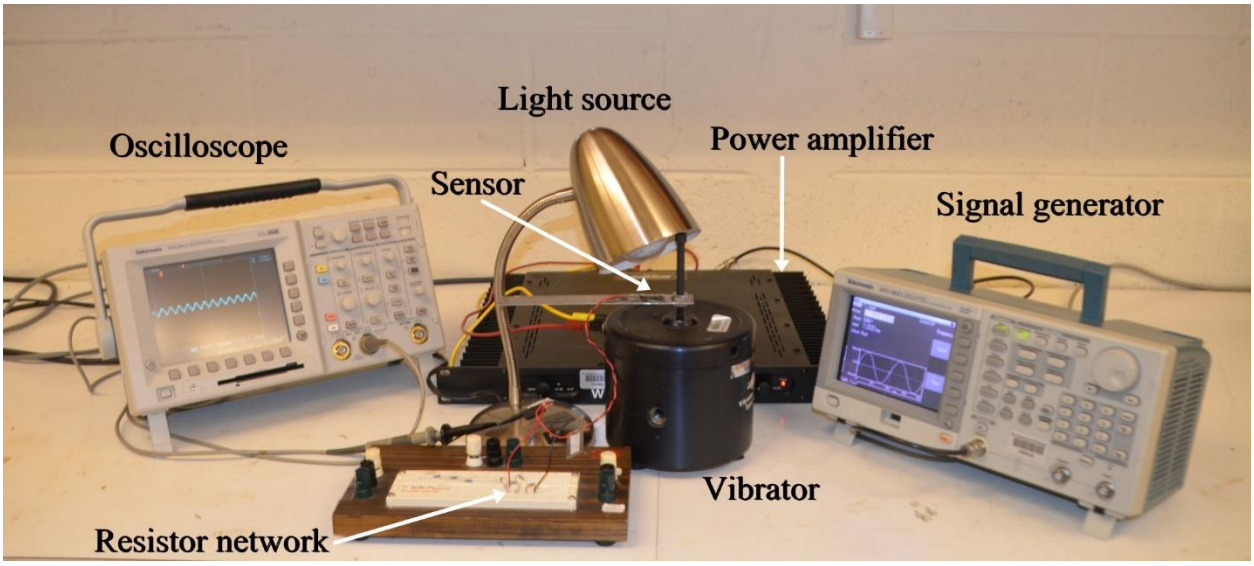

Figure 2.7 Actual setup of the experiment

2.4 Calibration:

2.4.1 Impedance Matching

In order to match the impedance of the circuit, various resistances used were 0.5, 0.75, 1 and 2 M ohm and the power output was compared at different frequencies for all four cases. Power output was calculated using the voltage output obtained for each individual frequency and was used to calculate the power output which was then plotted against the frequency range. Net power output, which is area under the curve of power and frequency was calculated using the trapezoidal rule.

The composition of nano-mixture used in this experiment was 59.9% Ferrofluid nanoparticles, 40% ZnO and 0.1% epoxy and three coated PZT substrates were connected in series over a rectangular plate and placed at a distance of 60 mm from the fixed end and excited from a frequency range of 65Hz to 700Hz

The output peak power and area under the curve was best achieved for the circuit resistance of 1 M Ohm that was 14140.59 µ Watt/sec. The power output for various circuit resistances under the frequency range of 65-700 Hz were compared, they are listed in Figure 2.8

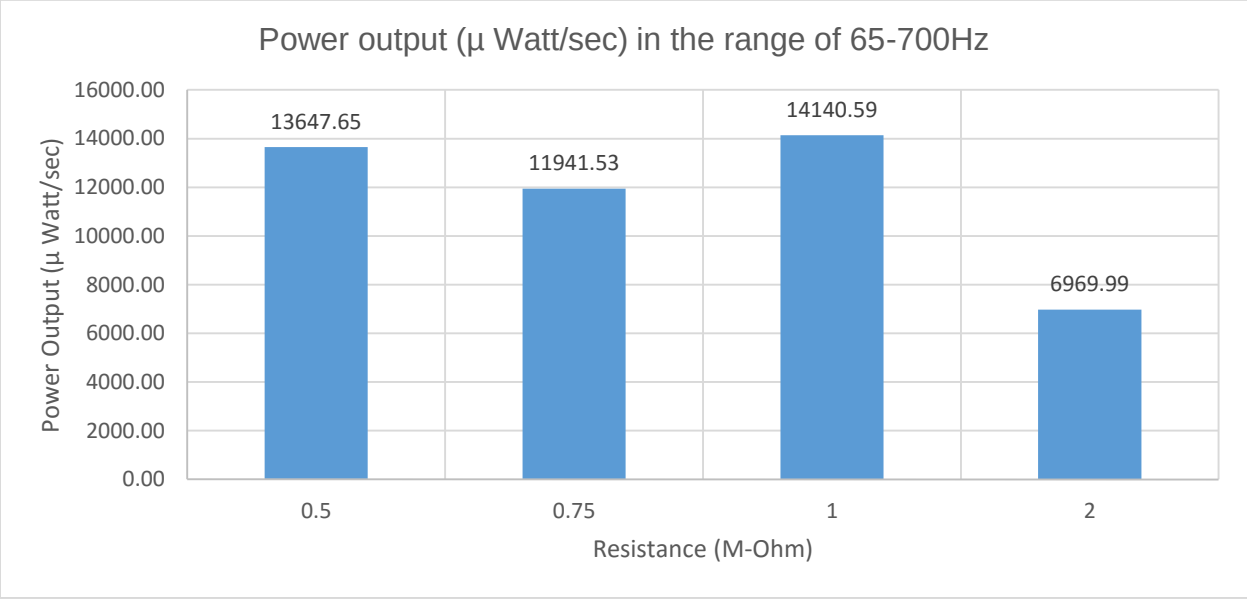

Figure 2.8 Impedance matching using power output comparison of PZT with Resistances in Mega-ohm excited in the frequency range of 65-700 HZ

After testing the external resistances of 0.5, 0.75, 1 and 2 M-Ohm, the best matched resistance value based on the area under power output-frequency of vibration was 1 M-Ohm in the frequency range of 65-700 Hz and it was 14140.59 µ Watt/sec.

2.4.2 Optimization of Epoxy

In order to optimize the amount of epoxy in the mixture, four solutions with different amount of epoxy were used. They were solution 1 (59.9% FNP, 40% ZnO and 0.1% epoxy), 2

(59.5% FNP, 40% ZnO and 0.5% epoxy), 3 (59% FNP, 40% ZnO and 1% epoxy) and 4 (59% FNP, 40% ZnO and 1% epoxy). All these solutions were excited at frequencies ranging from 65 Hz-400 Hz and the voltage output was used to calculate the power output and then plotted against the frequency range, the area under the curve was calculated using the trapezoidal rule. The comparison chart for 0.1% epoxy, 0.5% epoxy, 1% epoxy and 2% epoxy is shown in Figures 2.9.

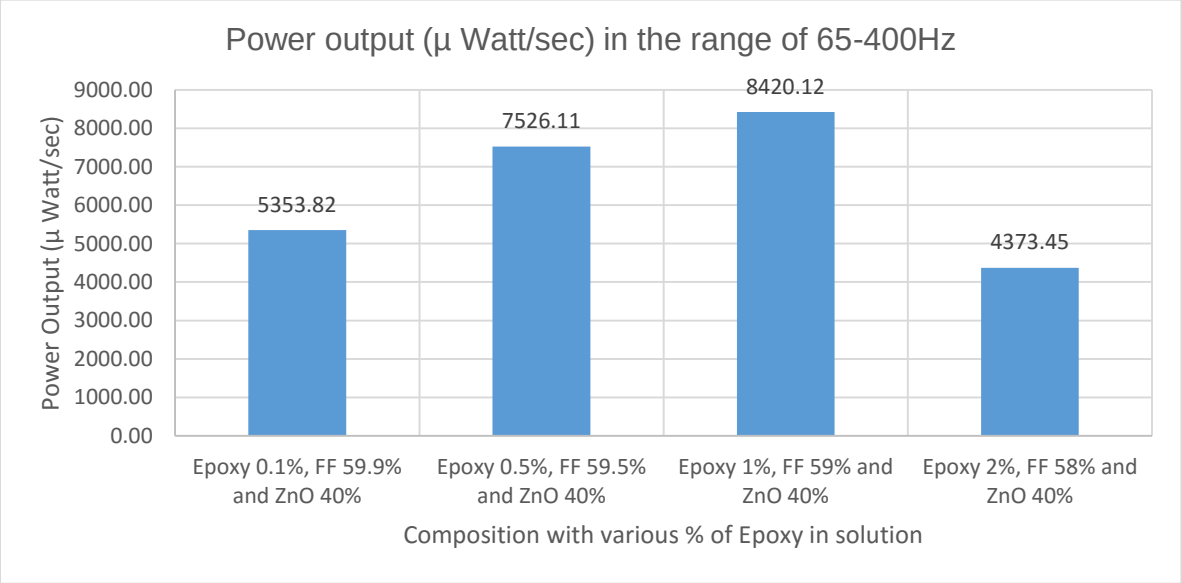

Figure 2.9 Epoxy optimization by comparing the power output of coated PZT with variation of Epoxy in Solution in the range of 65-400 HZ

Epoxy is the binding agent in the solution but the presence of epoxy can suppress the vibration in the substrate, which will reduce the power output hence the amount of epoxy was optimized and for this the content of epoxy was varied from 0.1, 0.5, 1 and 2% in the solution with keeping the amount of ZnO at 40% and varying the amount of Ferrofluid from 59.1, 59.5, 59 and 58% respectively. The area under the curve plotted between power output-frequency was compared and was found maximum for the solution 1% epoxy, 40% ZnO and 59% FNP and was found to be 8420.12 μ Watt/sec. in the frequency range of 65-400 Hz. Based on this conclusion all the samples had 1% epoxy in the resin solution that were carried out for the effect of graphene and light.

CHAPTER 3. COMPARISON OF COATING TECHNIQUE

3.1 Techniques Used

A brush coating technique and a spin coating technique were compared based on their power output in the frequency range of 65-400 Hz and the positioning of the fabricated PZT with different resin compositions were placed at a distance of 60mm from the free end.

3.2 Results and Discussion

The methods used earlier by Sudhanshu [58], Baghmar [57] and Nadeeka [61] were brush coating only which is not a scientific method hence a spin coating technique was adopted to compare the outcome with the brush coating technique. The brush coating results and the spin coated results are shown in Fligure 3.1.

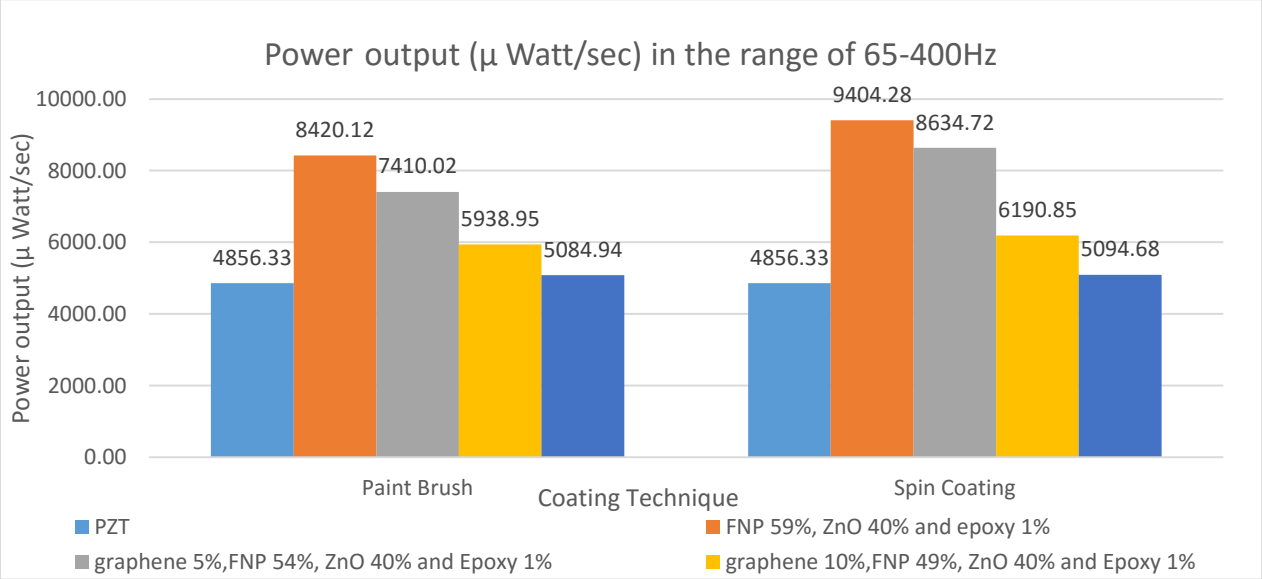

Figure 3.1 Comparison of power output of coated PZT with various compositions of nano-paste in the range of 65-400 HZ with different cases

Due to the presence of ZnO and graphene in the solution the output of the composite was increased with the increase in lumens and was found maximum for the substrate having solution graphene 5%, FNP 54%, ZnO 40% and epoxy 1% and with a value of 13279.23 µ watt/sec for 3780 lumens. There was an enhancement in substrate having different solution type under the influence of light with increasing lumens.

With the help of AFM, surface images of the substrates coated by different techniques were compared based on the surface texture and the distribution of the solution as in Figure 3.2.

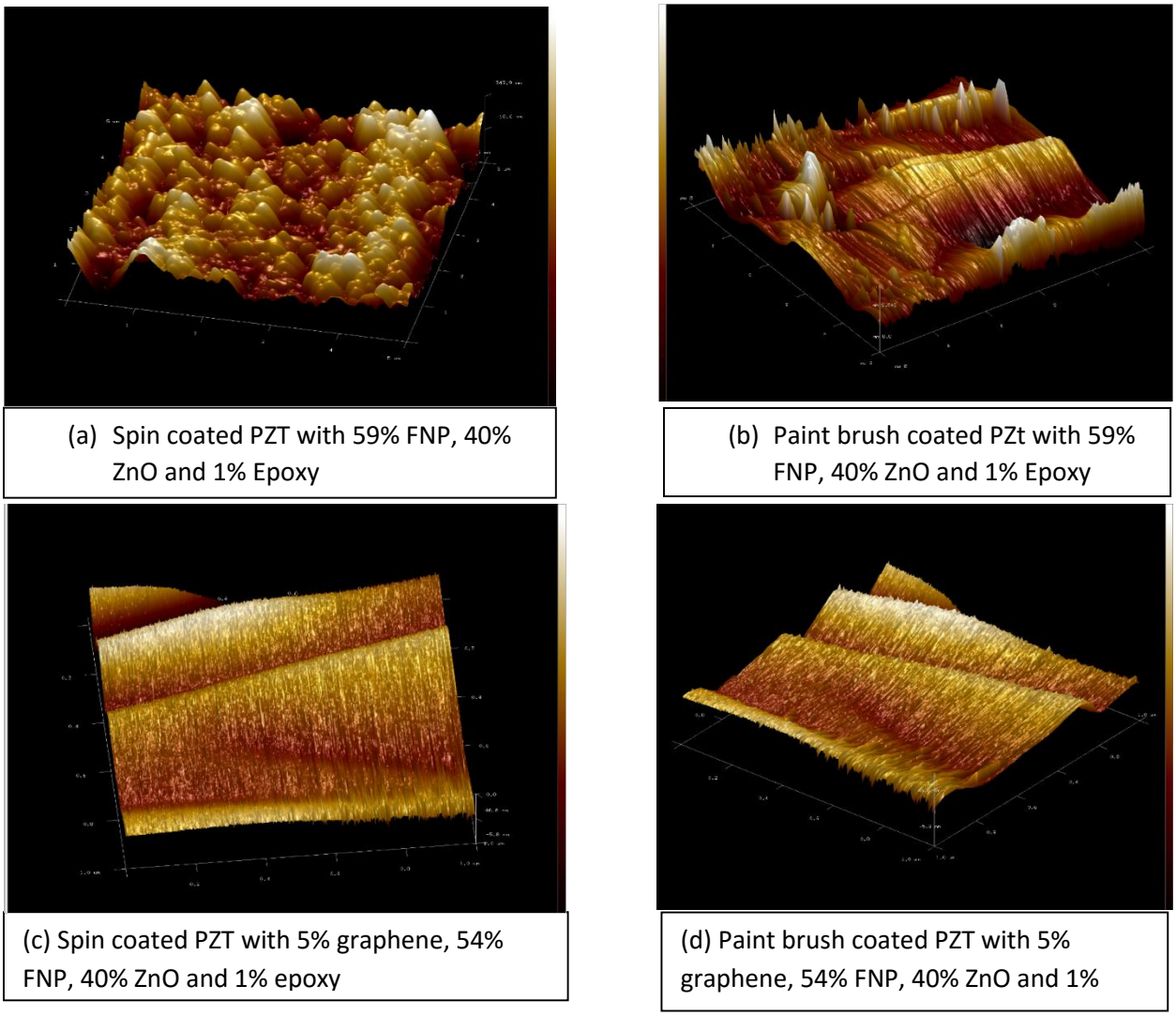

(a) Spin coated PZT with 59% FNP, 40% ZnO and 1% Epoxy

(b) Paint brush coated PZt with 59% FNP, 40% ZnO and 1% Epoxy

(c) Spin coated PZT with 5% graphene, 54% FNP, 40% ZnO and 1% epoxy

(d) Paint brush coated PZT with 5% graphene, 54% FNP, 40% ZnO and 1%

Figure 3.2 AFM images of coated PZT with various techniques

These composites were observed under Keyence VHX-2000 microscope (In Structures Lab, Mechanical Engineering) set at the magnification of 200x, as shown in Figure 3.3.

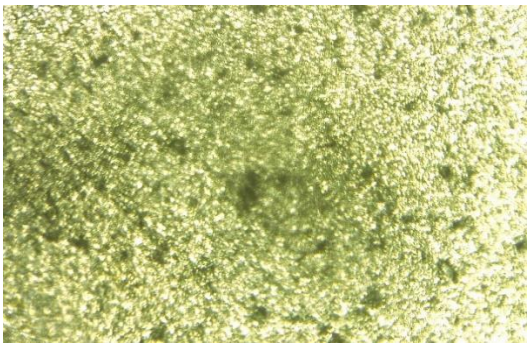

(a) PZT, 200X

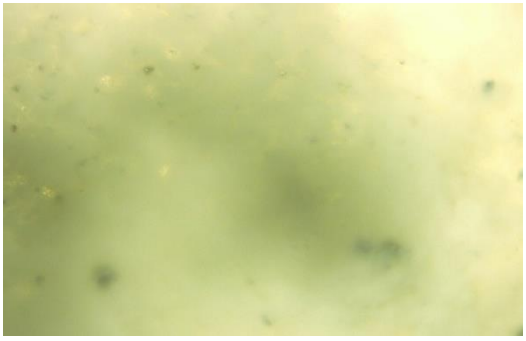

(b) nmp and ZnO over PZT, 200X

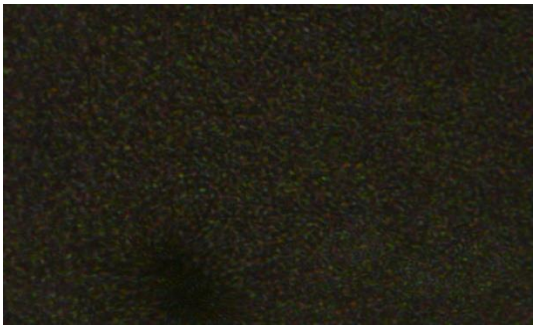

(c) nmp and graphene over PZT, 200X

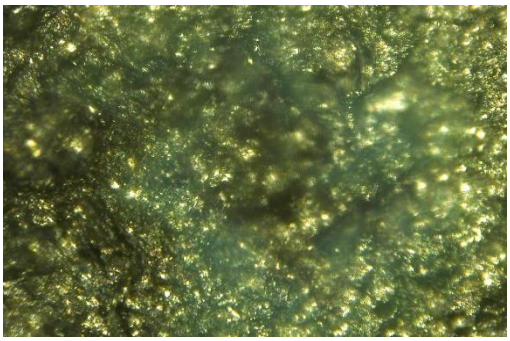

(d) Coated PZT with Nanopaste of Graphene, Ferrofluid, Zinc Oxide, 200X

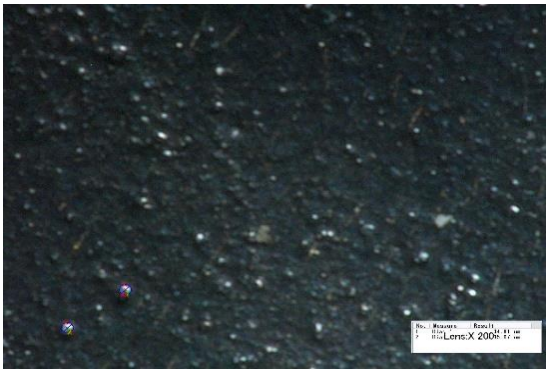

(e) FNP 59%, ZnO 40% and epoxy 1%, 200X

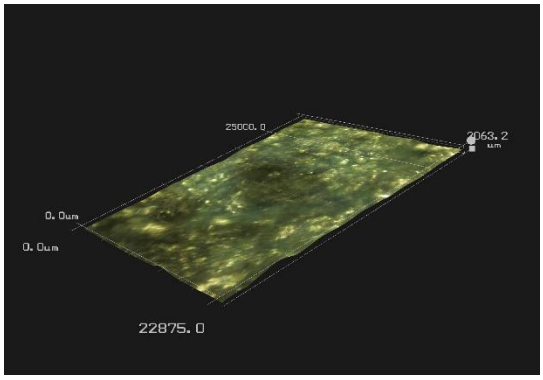

(f) 3-d image of spin coated PZT with a nanopaste of Graphene, Ferrofluid, Zinc Oxide and epoxy, 200X

Figure 3.3 Images of samples with microscope Keyence VHX-2000 (located in Structures lab in Mechanical Engineering)

The main reason to optimize the coating technique was repeatability and to find a better technique for getting an even resin (coating) layer on the PZT substrate. The techniques used were paint brush technique and spin coating technique, there was an increase in power output/sec for all the solutions prepared with the peaks being 8420.12 µ Watt/sec and 9404.28 µ Watt/sec for solution 1% epoxy, 40% ZnO and 59% FNP for brush coated and spin coated respectively. With the solution containing graphene, it was found that the peak was for the solution graphene 5%, FNP 54%, ZnO 40% and epoxy 1% having 7410.02 µ Watt/sec and 8634.72 µ Watt/sec respectively for brush coated and spin coated sensors under the frequency range of 65-400 Hz.

CHAPTER 4. EFFECT OF LIGHT

4.1 Effect of light (photovoltaic effect)

Nadeeka [61] studied the effect of light on her composite of PVDF having a coating of a mixture of ferrofluid and ZnO, hence an effort was made to study the effect of light (lumens) on the composite prepared. Graphene with ZnO acts as an efficient photocatalyst and was the motivation of studying the effect of light on the substrate. The sources used and their outcomes are shown in figures were 325 lumens, 565 lumens, 790 lumens, 1120 lumens, 2710 lumens, 3780 lumens

4.1.1 Effect of a light source of 325 lumens

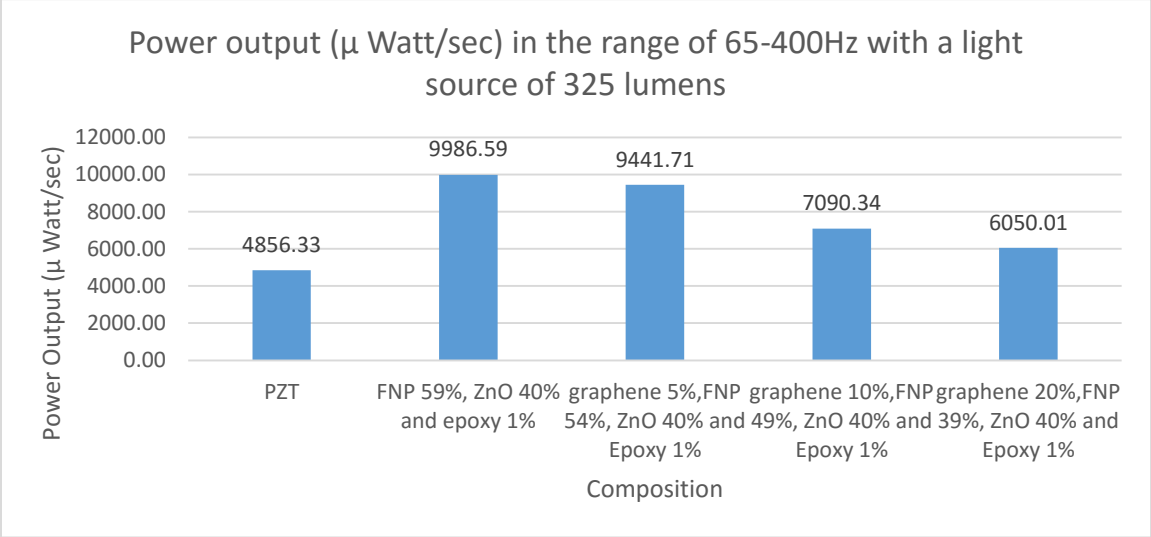

Figure 4.1 Comparison of power output of spin coated PZT with various compositions of nano-paste in the range of 65-400 HZ with a light source of 325 Lumens at a distance of 75mm

There was an increase of 6.2% for solution 1% epoxy, 40% ZnO and 59% FNP and an increase of 9.3% for solution graphene 5%, FNP 54%, ZnO 40% and epoxy 1% when compared

to vibration only. The details of output is listed in Figure 4.1.The maximum net power output was for 1% epoxy, 40% ZnO and 59% FNP followed by graphene 5%, FNP 54%, ZnO 40% and epoxy 1% which is roughly 6% less.

4.1.2 Effect of a light source of 565 lumens

There was an increase of 12.4% for solution 1% epoxy, 40% ZnO and 59% FNP and an increase of 18.85% for solution graphene 5%, FNP 54%, ZnO 40% and epoxy 1% when compared to vibration only. The maximum net power output was for 1% epoxy, 40% ZnO and 59% FNP followed by graphene 5%, FNP 54%, ZnO 40% and epoxy 1% which is roughly 3% less. Net power output is shown in Figure 4.2.

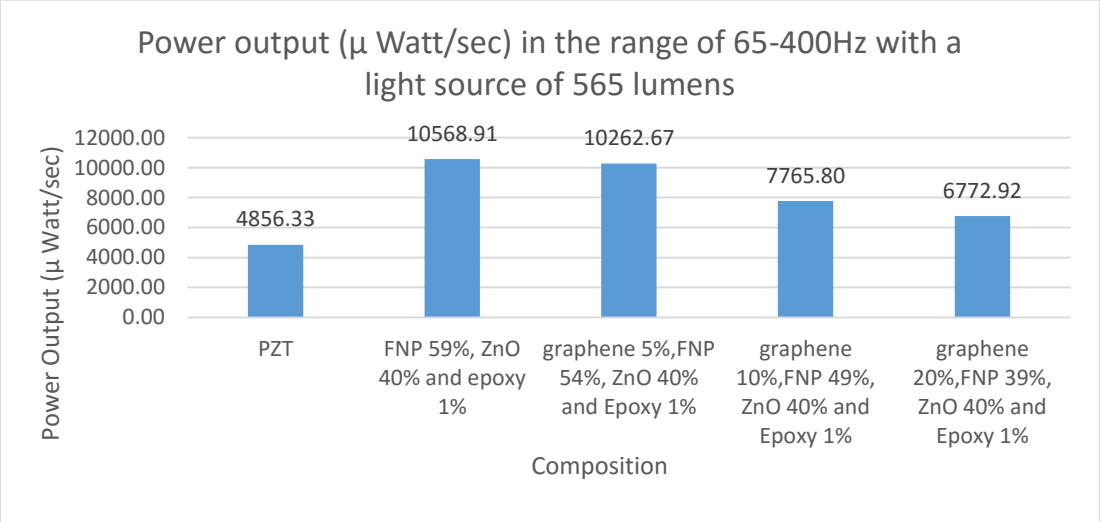

Figure 4.2 Comparison of power output of spin coated PZT with various compositions of nano-paste in the range of 65-400 HZ with a light source of 565 lumens at a distance of 75mm

4.1.3 Effect of a light source of 790 lumens

There was an increase of 18.7% for solution 1% epoxy, 40% ZnO and 59% FNP and an increase of 28% for solution graphene 5%, FNP 54%, ZnO 40% and epoxy 1% when compared to vibration only. The maximum net power output was for 1% epoxy, 40% ZnO and 59% FNP

followed by graphene 5%, FNP 54%, ZnO 40% and epoxy 1% which is roughly 0.8% less. As shown in Figure 4.3

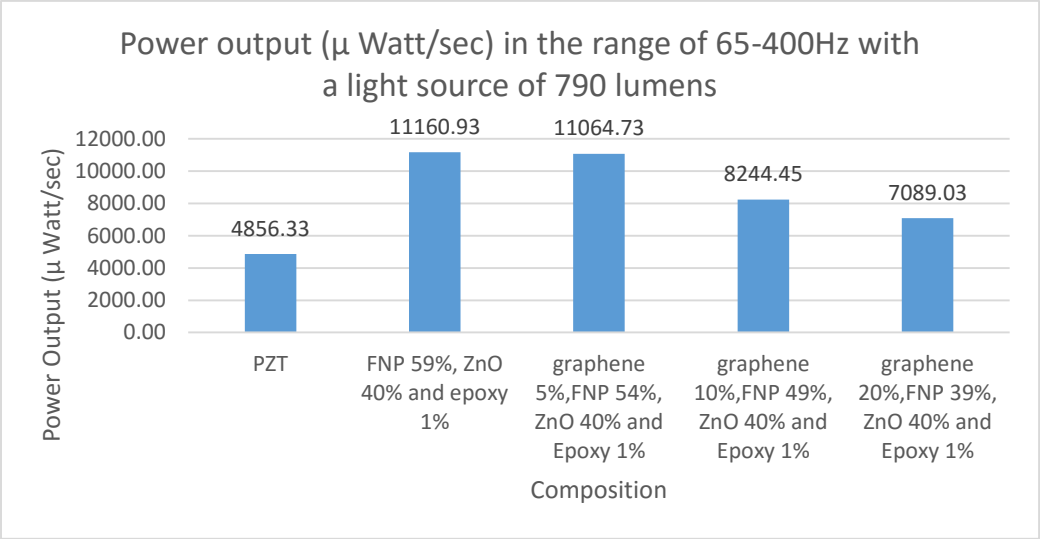

Figure 4.3 Comparison of power output of spin coated PZT with various compositions of nano-paste in the range of 65-400 HZ with a light source of 790 lumens at a distance of 75mm

4.1.4 Effect of a light source of 1120 lumens

There was an increase of 24% for solution 1% epoxy, 40% ZnO and 59% FNP and an increase of 36% for solution graphene 5%, FNP 54%, ZnO 40% and epoxy 1% when compared to vibration only. As shown in Figure 4.4

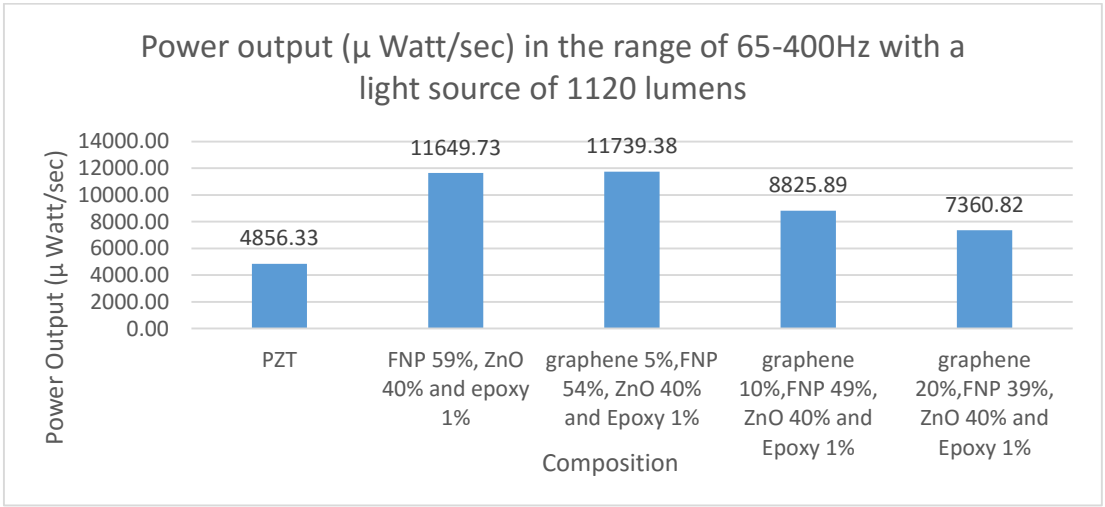

Figure 4.4 Comparison of power output of spin coated PZT with various compositions of nano-paste in the range of 65-400 HZ with a light source of 1120 lumens at a distance of 75mm

The maximum net power output was for graphene 5%, FNP 54%, ZnO 40% and epoxy 1% followed by 1% epoxy, 40% ZnO and 59% FNP which is roughly 0.8% less.

4.1.5 Effect of a light source of 2710 lumens

There was an increase of 31% for solution 1% epoxy, 40% ZnO and 59% FNP and an increase of 45% for solution graphene 5%, FNP 54%, ZnO 40% and epoxy 1% when compared to vibration only. The maximum net power output was for graphene 5%, FNP 54%, ZnO 40% and epoxy 1% followed by 1% epoxy, 40% ZnO and 59% FNP which is roughly 1.2% less. As shown in Figure 4.5.

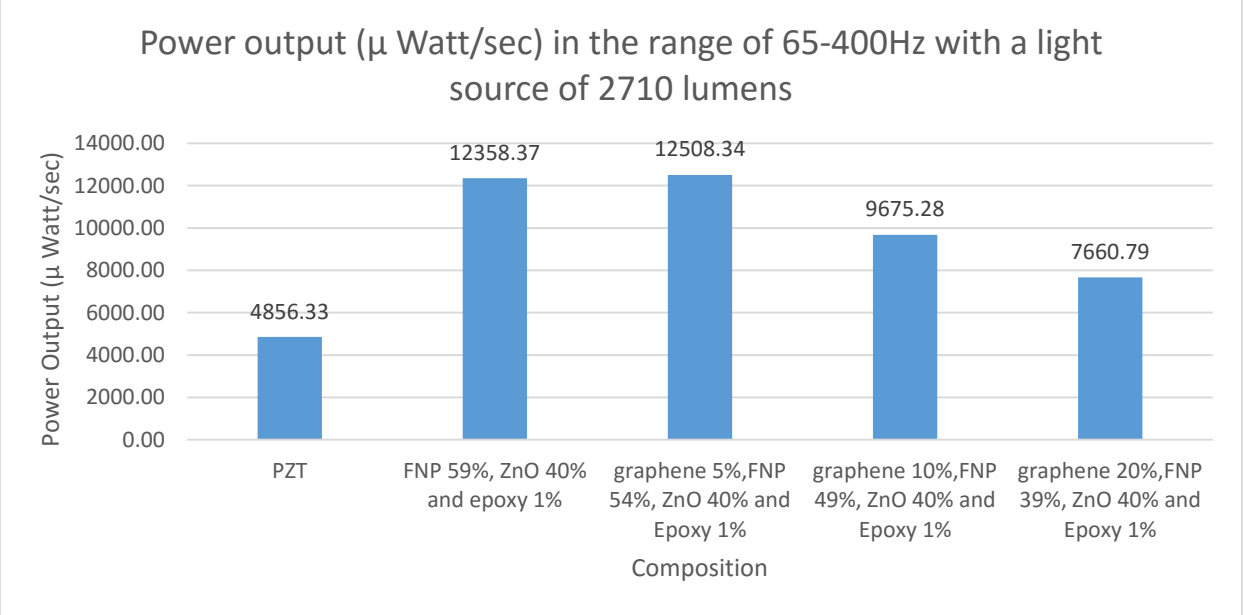

Figure 4.5 Comparison of power output of spin coated PZT with various compositions of nano-paste in the range of 65-400 HZ with a light source of 2710 Lumens at a distance of 75mm

4.1.6 Effect of a light source of 3780 lumens

There was an increase of 38% for solution 1% epoxy, 40% ZnO and 59% FNP and an increase of 54% for solution graphene 5%, FNP 54%, ZnO 40% and epoxy 1% when compared to vibration only. The maximum net power output was for graphene 5%, FNP 54%, ZnO 40% and

epoxy 1% followed by 1% epoxy, 40% ZnO and 59% FNP which is roughly 2% less. The results of power output is shown in Figure 4.6.

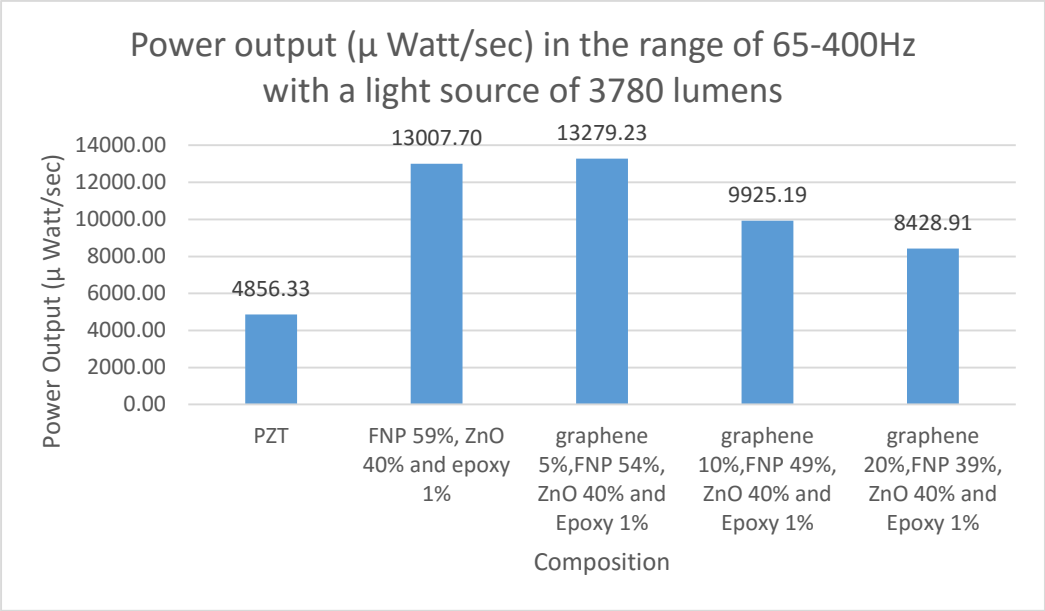

Figure 4.6 Comparison of power output of spin coated PZT with various compositions of nano-paste in the range of 65-400 HZ with a light source of 200W (3780 lumens) at a distance of 75mm

Due to the presence of ZnO and graphene in the solution the output of the composite was increased with the increase in lumens and was found maximum for the substrate having solution graphene 5%, FNP 54%, ZnO 40% and epoxy 1% and was 13279.23 µ watt/sec with 3780 lumens. There was an enhancement in substrate having different solution type under the influence of light with increasing lumens. The variation of net power output is shown in Figure 4.7.

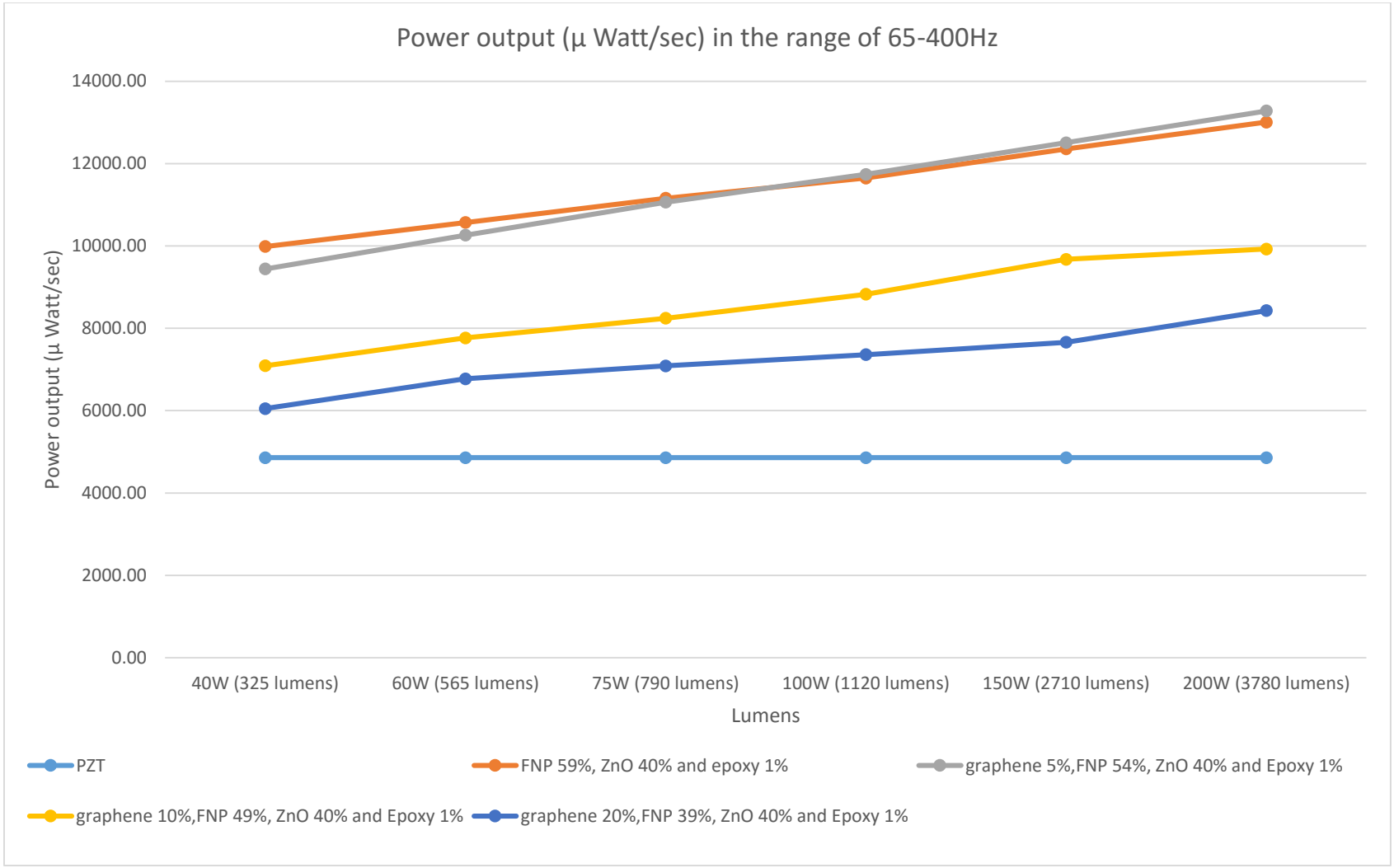

Figure 4.7 Comparison of power output of coated PZT with various compositions of nano-paste in the range of 65-400 Hz with different light sources.

4.2 Discussions

In this research three solutions were made with graphene in them. Solution 1 having graphene 5%, FNP 54%, ZnO 40% and Epoxy 1%, solution 2 having graphene 10%, FNP 49%, ZnO 40% and Epoxy 1% and solution 3 having graphene 20%, FNP 39%, ZnO 40% and Epoxy 1% was coated on PZT substrate. The net power output was compared based on area under the curve plotted between power output-frequency. The maximum power/sec (µ Watt/sec) was found to be 7410.02 µ Watt/sec for solution graphene 5%, FNP 54%, ZnO 40% and Epoxy 1% under the frequency range of 65-400 Hz.

The effect of light was recorded and the light sources used were 325 lumens, 565 lumens790 lumens, 1120 lumens, 2710 lumens and 3780 lumens. Due to the presence of ZnO and graphene in the solution, which acts as an efficient photocatalyst [19], the output of the composite was increased with the increase in lumens and was found maximum for the substrate having solution graphene 5%, FNP 54%, ZnO 40% and Epoxy 1% and was 13279.23 µ Watt/sec with 3780 lumens.

CHAPTER 5. CONCLUSIONS, DISCUSSIONS AND FUTURE WORK

5.1 Coating Technique

Earlier Baghmar [57], Sudhanshu [58] and Nadeeka [61] used a paint brush approach to coat the piezo surface. This is not a scientific method and there can my numerous limitations with this technique is repeatability being one of them. Due to repeatability and uniformity of coating a spin coating technique was used to resolve both these issues. Comparing the results there was an increase in peaks, the power was 8420.12 µ Watt/sec and 9404.28 µ Watt/sec for the solution of 1% epoxy, 40% ZnO and 59% FNP for brush coated and spin coated respectively. With the solution containing graphene, it was found that the peak was for solution with graphene 5%, FNP 54%, ZnO 40% and Epoxy 1% having 7410.02 µ Watt/sec and 8634.72 µ Watt/sec respectively for brush coated and spin coated sensors under the frequency range of 65-400 Hz.

5.2 Power Output with addition of graphene and light effect

There was not a significant change, in fact the output degraded with the addition of graphene. The main reason behind this decrease or no improvement is because graphene does not have any piezoelectric effect. The maximum power output in the range of 65-400 Hz was for 9404.28 µ Watt/sec for the solution of 1% epoxy, 40% ZnO and 59% FNP while opting for the spin-coating technique. Although, there was an increase in power output when the substrate was exposed to light and the substrate with 5% graphene on got the best out of it with an additional effect of vibrations. Graphene possess excellent photovoltaic properties, this was the reason the

output in 65-400Hz was found maximum for the substrate having solution graphene 5%, FNP 54%, ZnO 40% and epoxy 1% and was 13279.23 µ Watt/sec with 3780 lumens which is 1.02% and 173% more than compared to FNP 59%, ZnO 40% and epoxy 1% 13007.70 µ Watt/sec and PZT 4856.33 µ Watt/sec respectively. The main reason behind this increase in power output was the zero-gap semiconductor [43] property of graphene which basically acted as a solar dye [47-49] which in addition to the vibrational energy also converts the available light energy.

5.3 Future Work Suggestions

The basic goal of this work was to study the effect of light and vibrations on a piezo material having a coating of material with photovoltaic properties. Future work should be:

1. Testing different photovoltaic materials used.
2. The coating technique that involves the deposition of a photovoltaic material over the piezo material should optimized further by varying the parameters (time, speed and acceleration) used in the spin coating technique by studying the viscosity, drying rate and surface tension of the mixture.
3. The type of piezoelectric materials used should be focused more on polymers, since they have more diverse applications.

LIST OF REFERENCES

[1] Roundy, S., and Y. Zhang (2005), Toward self-tuning adaptive vibration based micro-generator, *Sydney , Australia, 16*, 373–384.

[2] Shen, D. (2009), "Piezoelectric energy harvesting devices for low frequency vibration applications." *Ph.D. thesis, Auburn University, Auburn, Alabama.*

[3] https://en.wikipedia.org/wiki/Piezoelectricity

[4] http://www.explainthatstuff.com/piezoelectricity.html

[5] Sodano, Henry A., Daniel J. Inman, and Gyuhae Park. "Comparison of piezoelectric energy harvesting devices for recharging batteries." *Journal of Intelligent Material Systems and Structures* 16.10 (2005): 799-807.

[6] Cook-Chennault, K. A., N. Thambi, and A. M. Sastry. "Powering MEMS portable devices—a review of non-regenerative and regenerative power supply systems with special emphasis on piezoelectric energy harvesting systems." *Smart Materials and Structures* 17.4 (2008): 043001.

[7] Anton, Steven R., and Henry A. Sodano. "A review of power harvesting using piezoelectric materials (2003–2006)." *Smart materials and Structures* 16.3 (2007): R1.

[8] Wu, Weiwei, et al. "Lead zirconate titanate nanowire textile nanogenerator for wearable energy-harvesting and self-powered devices." *ACS nano* 6.7 (2012): 6231-6235.

[9] Scaparo, Justin, and Tolga Kaya. "Piezoelectric energy harvester design and fabrication." *Proceedings of the 2012 ASEE North Central Section Conference*. 2012.

[10] Wang, Zhong Lin, and Jinhui Song. "Piezoelectric nanogenerators based on zinc oxide nanowire arrays." *Science* 312.5771 (2006): 242-246..

[11] Kwok, Chi Kong, and Seshu B. Desu. "Low temperature perovskite formation of lead zirconate titanate thin films by a seeding process." *Journal of materials research* 8.02 (1993): 339-344.

[12] Wang, Zhan Jie, et al. "Crystal structure and microstructure of lead zirconate titanate (PZT) thin films with various Zr/Ti ratios grown by hybrid processing."*Journal of crystal growth* 267.1 (2004): 92-99.

[13] http://large.stanford.edu/courses/2012/ph240/garland1/

[14] http://www.comsol.com/blogs/piezoelectric-materials-crystal-orientation-poling-direction/

[15] Paradiso, Joseph A., and Thad Starner. "Energy scavenging for mobile and wireless electronics." *Pervasive Computing, IEEE* 4.1 (2005): 18-27.

[16] Mitcheson, Paul D., et al. "Energy harvesting from human and machine motion for wireless electronic devices." *Proceedings of the IEEE* 96.9 (2008): 1457-1486.

[17] Sodano, Henry A., Daniel J. Inman, and Gyuhae Park. "Comparison of piezoelectric energy harvesting devices for recharging batteries." *Journal of Intelligent Material Systems and Structures* 16.10 (2005): 799-807.

[18] Cook-Chennault, K. A., N. Thambi, and A. M. Sastry. "Powering MEMS portable devices—a review of non-regenerative and regenerative power supply systems with special emphasis on piezoelectric energy harvesting systems." *Smart Materials and Structures* 17.4 (2008): 043001.

[19] Xu, Tongguang, et al. "Significantly enhanced photocatalytic performance of ZnO via graphene hybridization and the mechanism study." *Applied Catalysis B: Environmental* 101.3 (2011): 382-387.

[20] Lü, Kui, GuiXia Zhao, and XiangKe Wang. "A brief review of graphene-based material synthesis and its application in environmental pollution management." *Chinese Science Bulletin* 57.11 (2012): 1223-1234.

[21] Chen, Sheng, Junwu Zhu, and Xin Wang. "An in situ oxidation route to fabricate graphene nanoplate–metal oxide composites." *Journal of Solid State Chemistry*184.6 (2011): 1393-1399.

[22] Beeby, S. P, M. J Tudor, and N. M. White. "Energy harvesting vibration sources for microsystems applications." *Measurement science and technology* 17.12 (2006): R175.

[23] Muralt, Paul. "PZT thin films for microsensors and actuators: Where do we stand?" *Ultrasonics, Ferroelectrics, and Frequency Control, IEEE Transactions on* 47.4 (2000): 903-915.

[24] Balma, Robert, and Tolga Kaya. "Battery-Free Energy Scavenging Applications and Power Conditioning Circuit." *American Society for Engineering Education (Asee)* (2012).

[25] Sharma, Bhupendra K., et al. "Study of intermediate states in shape transition of ZnO nanostructures from nanoparticles to nanorods." *Chemical Physics Letters* 515.1 (2011): 62-67.

[26] Schmidt-Mende, Lukas, and Judith L. MacManus-Driscoll. "ZnO–nanostructures, defects, and devices." *Materials today* 10.5 (2007): 40-48.

[27] Wang, Zhong Lin, and Jinhui Song. "Piezoelectric nanogenerators based on zinc oxide nanowire arrays." *Science* 312.5771 (2006): 242-246.

[28] Chen, Xi, et al. "1.6 V nanogenerator for mechanical energy harvesting using PZT nanofibers." *Nano letters* 10.6 (2010): 2133-2137.

[29] Kwon, Junggou, Bhupendra K. Sharma, and Jong-Hyun Ahn. "Graphene Based Nanogenerator for Energy Harvesting." *Japanese Journal of Applied Physics*52.6S (2013): 06GA02.

[30] Zhu, Guang, et al. "Flexible high-output nanogenerator based on lateral ZnO nanowire array." *Nano letters* 10.8 (2010): 3151-3155.

[31] Lin, Long, et al. "Transparent flexible nanogenerator as self-powered sensor for transportation monitoring." *Nano Energy* 2.1 (2013): 75-81.

[32] Chang, Chieh, et al. "Direct-write piezoelectric polymeric nanogenerator with high energy conversion efficiency." *Nano letters* 10.2 (2010): 726-731.

[33] Kwon, Junggou, et al. "A high performance PZT ribbon-based nanogenerator using graphene transparent electrodes." *Energy Environ. Sci.* 5.10 (2012): 8970-8975.

[34] Wu, Weiwei, et al. "Lead zirconate titanate nanowire textile nanogenerator for wearable energy-harvesting and self-powered devices." *ACS nano* 6.7 (2012): 6231-6235.

[35] Lee, Keun Young, et al. "P-Type polymer-hybridized high-performance piezoelectric nanogenerators." *Nano letters* 12.4 (2012): 1959-1964.

[36] Bachari, E. M., et al. "Structural and optical properties of sputtered ZnO films." *Thin Solid Films* 348.1 (1999): 165-172.

[37] Özgür, Ü. et al. "A comprehensive review of ZnO materials and devices." *Journal of applied physics* 98.4 (2005): 041301.

[38] Wang, Z. L. (2011), From nanogenerators to piezotronicsa decade-long study of zno nanostructures, *Lecture 2012.186*, MRS. 1, 3, 22

[39] Zhao, Min-Hua, Zhong-Lin Wang, and Scott X. Mao. "Piezoelectric characterization of individual zinc oxide nanobelt probed by piezoresponse force microscope." *Nano Letters* 4.4 (2004): 587-590.

[40] Zahn, Markus. "Magnetic fluid and nanoparticle applications to nanotechnology." *Journal of Nanoparticle Research* 3.1 (2001): 73-78.

[41] Odenbach, Stefan, and Steffen Thurm. "Magnetoviscous effects in ferrofluids." *Springer Berlin Heidelberg*, 2002.

[42] P Berger, et al. "Preparation and properties of an aqueous ferrofluid." *Journal of Chemical Education* 76, no. 7 (1999): 943.

[43] Chandratre, Swapnil, and Pradeep Sharma. "Coaxing graphene to be piezoelectric." *Applied Physics Letters* 100.2 (2012): 023114.

[44] Geim, Andre K., and Konstantin S. Novoselov. "The rise of graphene." *Nature materials* 6.3 (2007): 183-191.

[45] Wang, Yan, et al. "Supercapacitor devices based on graphene materials." *The Journal of Physical Chemistry C* 113.30 (2009): 13103-13107.

[46] Chandratre, Swapnil, and Pradeep Sharma. "Coaxing graphene to be piezoelectric." *Applied Physics Letters* 100.2 (2012): 023114.

[47] Wan, Xiangjian, et al. "Graphene–a promising material for organic photovoltaic cells." *Advanced Materials* 23.45 (2011): 5342-5358.

[48] Liu, Zunfeng, et al. "Organic photovoltaic devices based on a novel acceptor material: graphene." *Adv. Mater* 20.20 (2008): 3924-3930.

[49] Liu, Qian, et al. "Organic photovoltaic cells based on an acceptor of soluble graphene." *Applied Physics Letters* 92.22 (2008): 223303.

[50] Beeby, S. P, M. J Tudor, and N. M. White. "Energy harvesting vibration sources for microsystems applications." *Measurement science and technology*17.12 (2006): R175.

[51] Wang, Zhong Lin, and Jinhui Song. "Piezoelectric nanogenerators based on zinc oxide nanowire arrays." *Science* 312.5771 (2006): 242-246.

[52] Wang, Zhihong, et al. "Dense PZT thick films derived from sol-gel based nanocomposite process." *Materials Science and Engineering: B* 99.1 (2003): 56-62.

[53] Scaparo, Justin, and Tolga Kaya. "Piezoelectric energy harvester design and fabrication." *Proceedings of the 2012 ASEE North Central Section Conference*. 2012.

[54] Cernea, M., et al. "Synthesis of La and Nb doped PZT powder by the gel-combustion method." *Nanotechnology* 17.6 (2006): 1731.

[55] Zavala, Genaro, Janos H. Fendler, and Susan Trolier-McKinstry. "Characterization of ferroelectric lead zirconate titanate films by scanning force microscopy." *Journal of Applied Physics* 81.11 (1997): 7480-7491.

[56] Veeregowda, D.H., "Tribo acoustics tool for stick slip friction and energy harvesting using nanoparticles*" Thesis*, 2007.

[57] Bhagmar, S. *"*Patterned NANO coated energy harvester composites from vibration*" Thesis,* 2009.

[58] Sharma, S. "Smart nanocoated structure for energy harvesting at low frequency vibration" *Thesis*, 2011.

[59] R.N.Torah, S.P.Beeby, M. Tudor, T.ODonnell, and S.Roy (2006), "Development of a cantilever beam generator employing vibration energy harvesting", *Conference item*, University of Southampton.

[60] Murata USA - http://www.murata.com/products/catalog/pdf/p37e.pdf.

[61] Karunarathna, N. "Enhanced pvdf film for multi energy harvesting" *Thesis*, 2013.

LIST OF APPENDICES

APPENDIX A: GENERAL INFORMATION

Calculation of power:

With the help of Oscilloscope the output root mean square voltage was determined then the relation between power, voltage and resistance was used.

$$P = V_{rms}^2/R$$

Where P is power in watt, V_{rms} is root mean square voltage in volts, and R is resistance in ohm.

Calculation of Area under the curve by Trapezoidal Rule in excel:

When the function f(x) is not known, or it cannot be evaluated analytically, the above integral should be determined numerically. This can be done in a number of ways, some of which are better than others. The ***trapezoidal rule*** is one of the best ways to calculate this integral its advantages over other methods are (1) easy to implement; (2) accurate; and (3) quite robust. The technique is to break the function up into numerous trapezoids and calculate the individual areas.

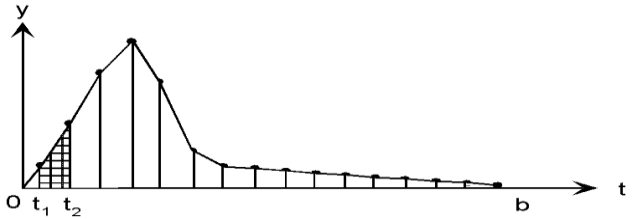

Figure 0.1 sample curve for calculation of area under the curve

The area of the shaded trapezoid above is

$$Area = \left(t_2 - t_1\right)\left[\frac{f\left(t_1\right) + f\left(t_2\right)}{2}\right]$$

The area under the graph is therefore the sum of the area of all the trapezoids. The accuracy of the numerical integration will go up with decreased spacing between the time points. That's why an effort was made to get as more spacing as a result 17 spacing's were considered in a frequency interval from 60-400 Hz.

APPENDIX B: POWER OUTPUT CURVES

Optimization of Epoxy

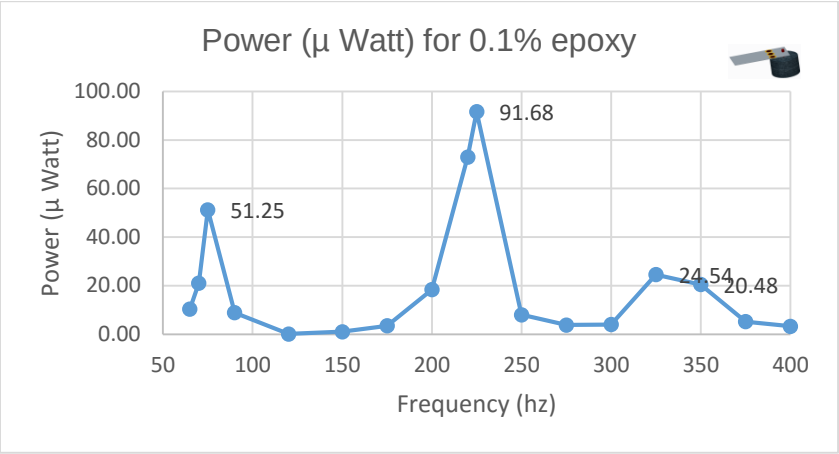

Figure 0.2 Power output of nano-coated PZT having 0.1% epoxy from frequency range of 65-400 Hz

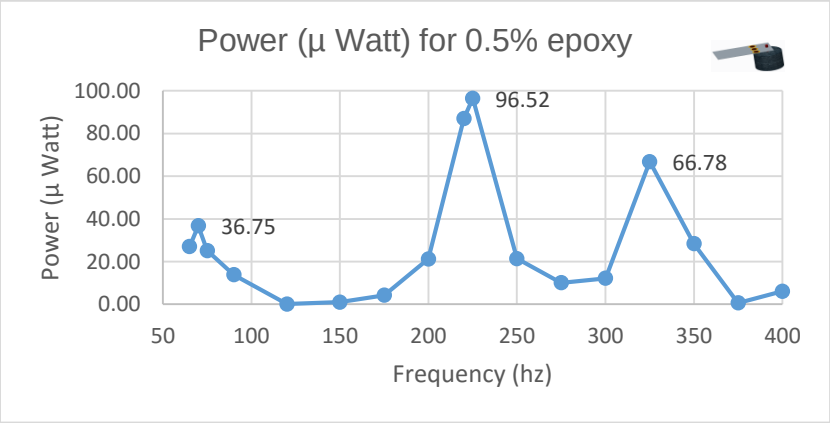

Figure 0.3 Power output of nano-coated PZT having 0.5% epoxy from frequency range of 65-400 HZ

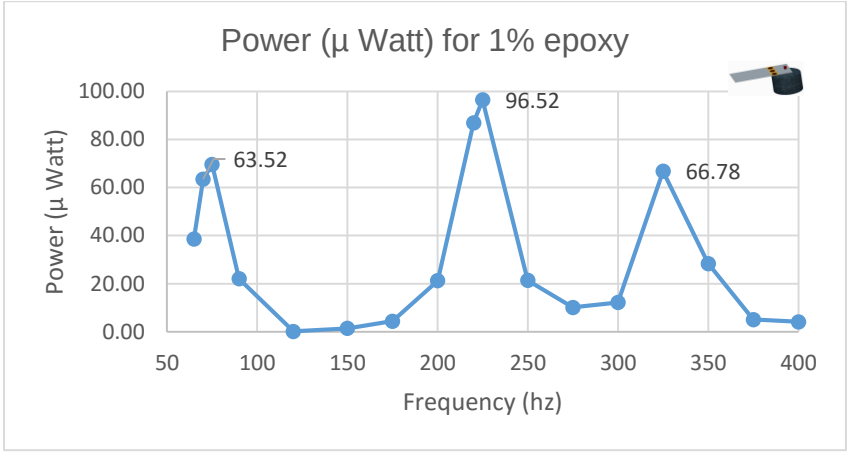

Figure 0.4 Power output of nano-coated PZT having 1% epoxy from frequency range of 65-400 HZ

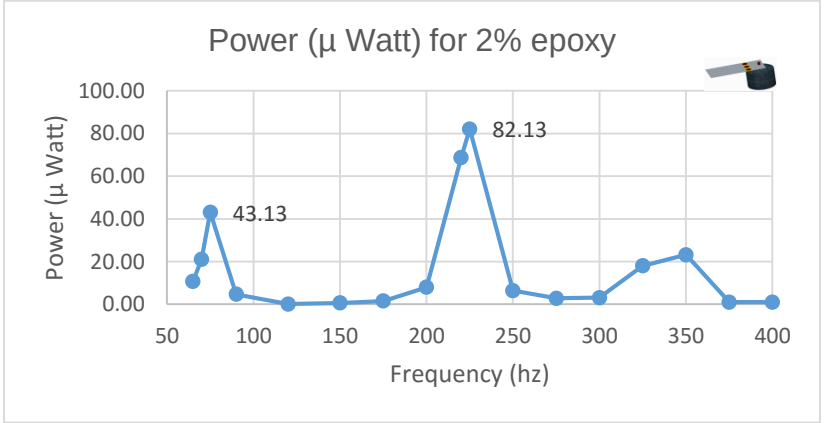

Figure 0.5 Power output of nano-coated PZT having 2% epoxy from frequency range of 65-400 HZ

Brush Coated Results

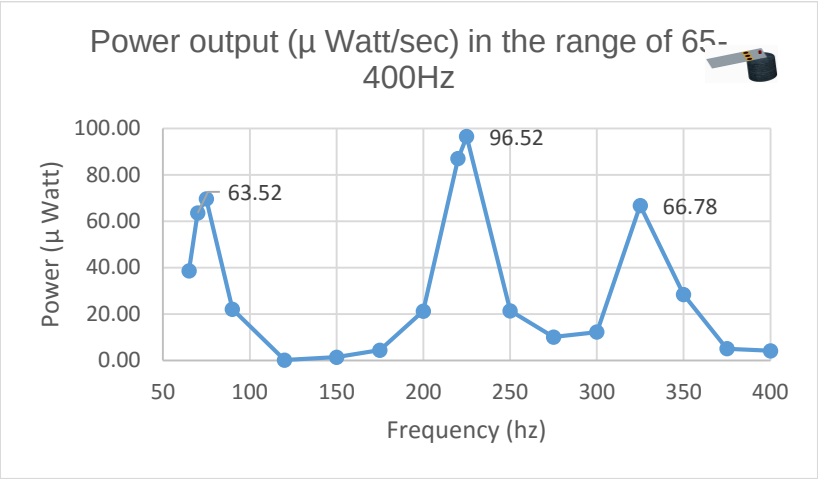

Figure 0.6 Power output of PZT with brush coated FNP 59%, ZnO 40% and epoxy 1%

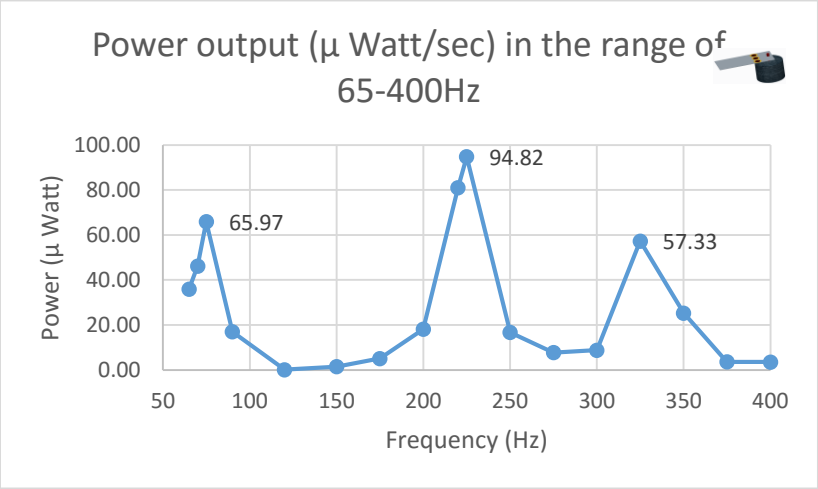

Figure 0.7 Power output of PZT with brush coated graphene 5%, FNP 54%, ZnO 40% and epoxy 1%

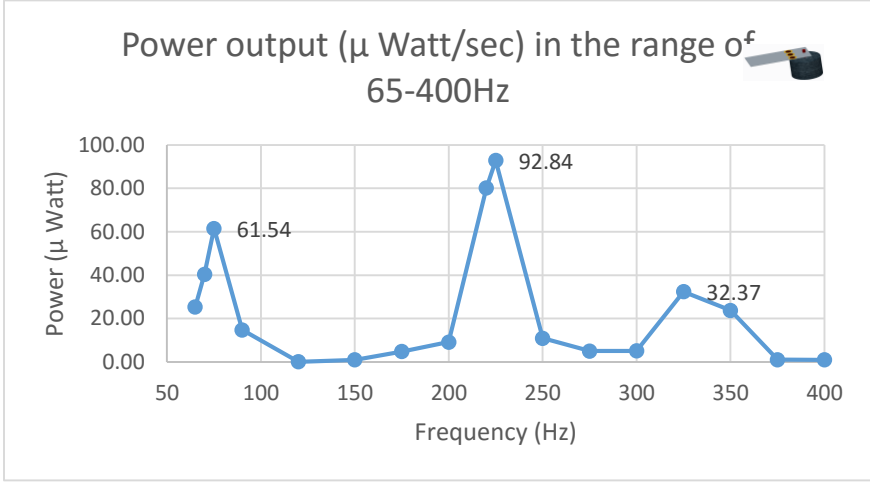

Figure 0.8 Power output of PZT with brush coated graphene 10%, FNP 49%, ZnO 40% and epoxy 1%

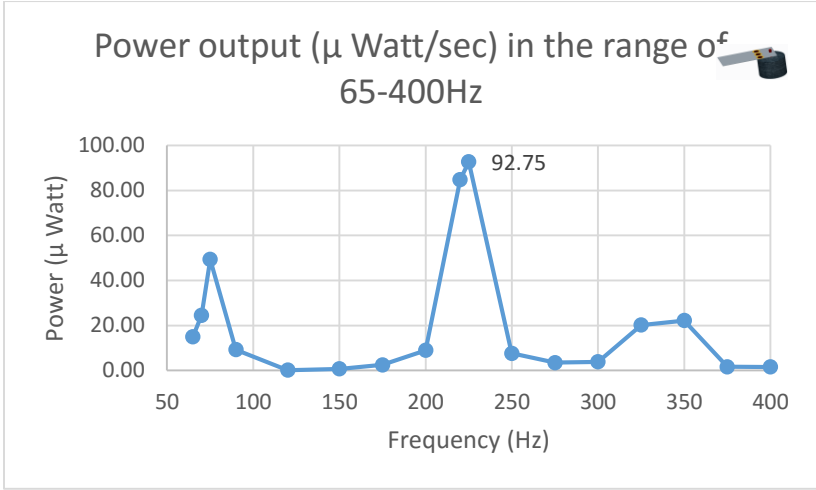

Figure 0.9 Power output of PZT with brush coated graphene 20%, FNP 39%, ZnO 40% and epoxy 1%

Spin Coating Results

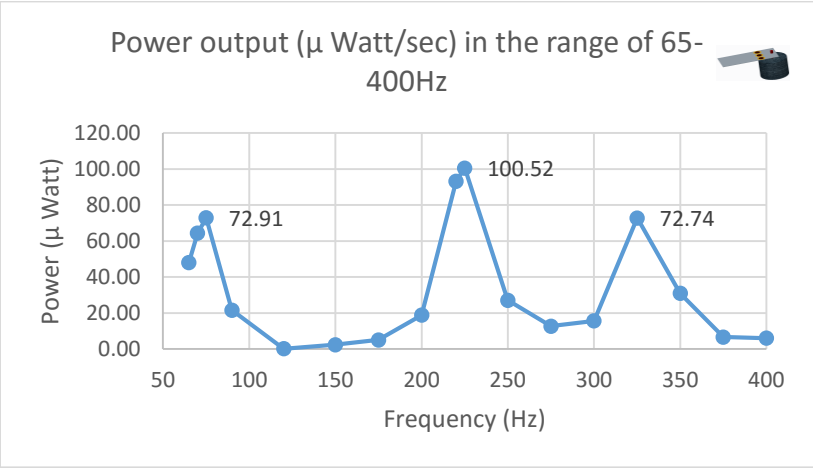

Figure 0.10 Power output of PZT with spin coated graphene 5%, FNP 54%, ZnO 40% and epoxy 1%

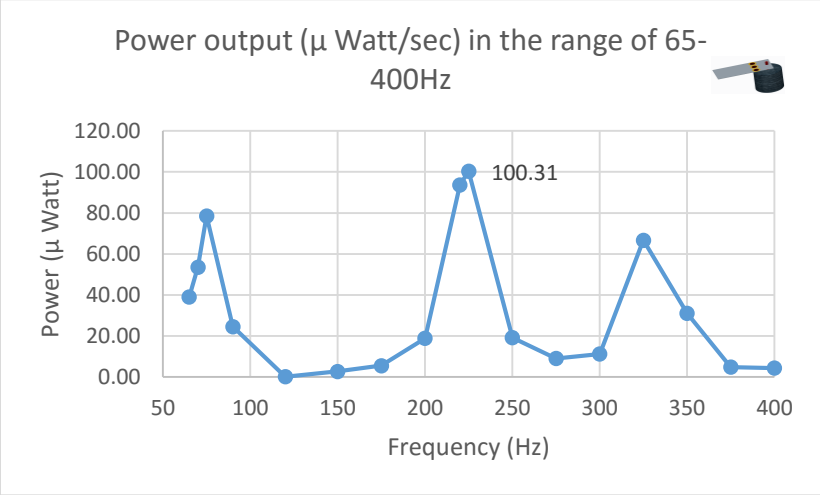

Figure 0.11 Power output of PZT with spin coated PZT with FNP 59%, ZnO 40% and epoxy 1%

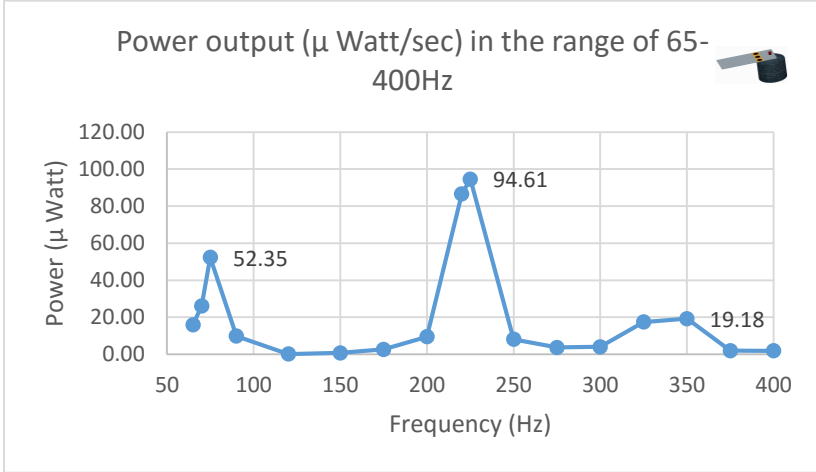

Figure 0.12 Power output of PZT with spin coated graphene 20%, FNP 39%, ZnO 40% and epoxy 1%

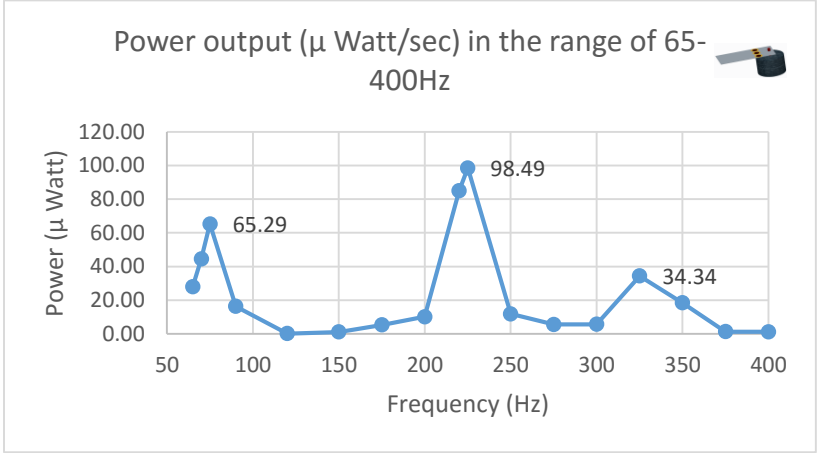

Figure 0.13 Power output of PZT with spin coated graphene 10%, FNP 49%, ZnO 40% and epoxy 1%

Effect of Light

Results under light source of 325 lumens

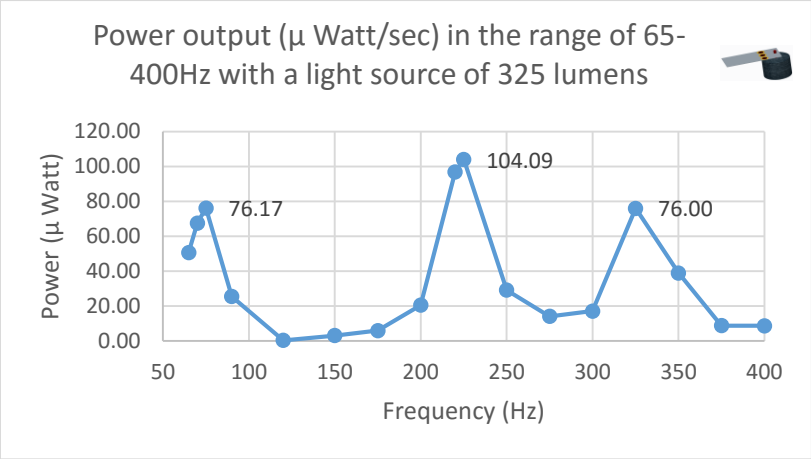

Figure 0.14 Power output of PZT with spin coated PZT with FNP 59%, ZnO 40% and epoxy 1%

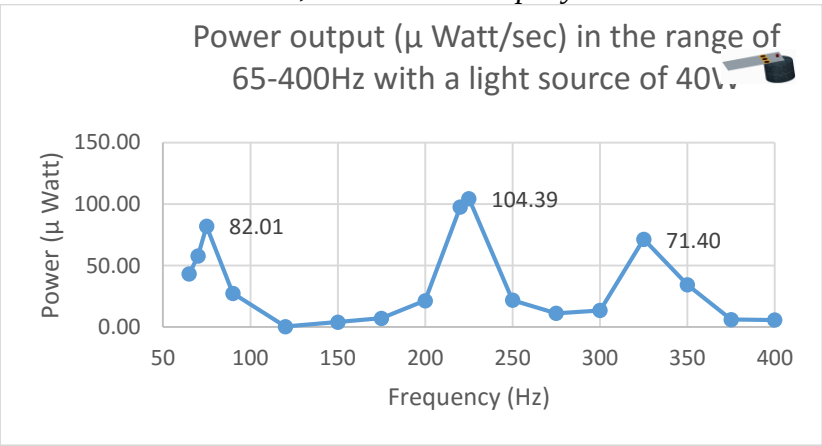

Figure 0.15 Power output of PZT with spin coated graphene 5%, FNP 54%, ZnO 40% and epoxy 1%

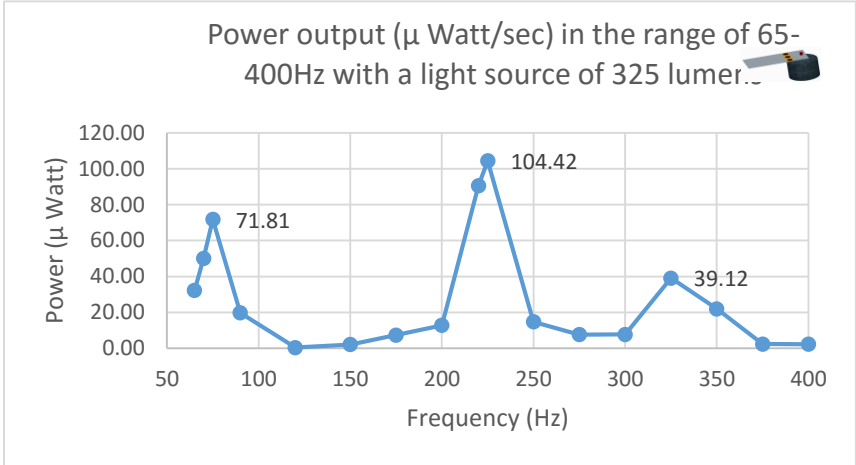

Figure 0.16 Power output of PZT with spin coated graphene 10%, FNP 49%, ZnO 40% and epoxy 1%

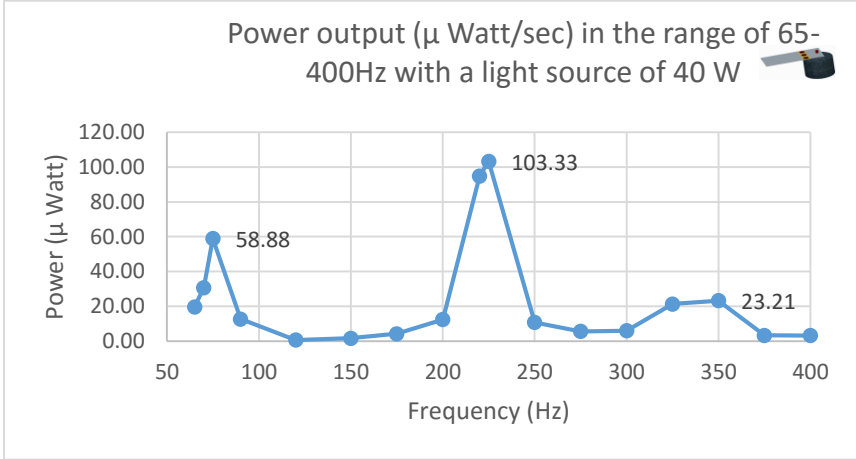

Figure 0.17 Power output of PZT with spin coated graphene 20%, FNP 39%, ZnO 40% and epoxy 1%

Results under light source of 565 lumens

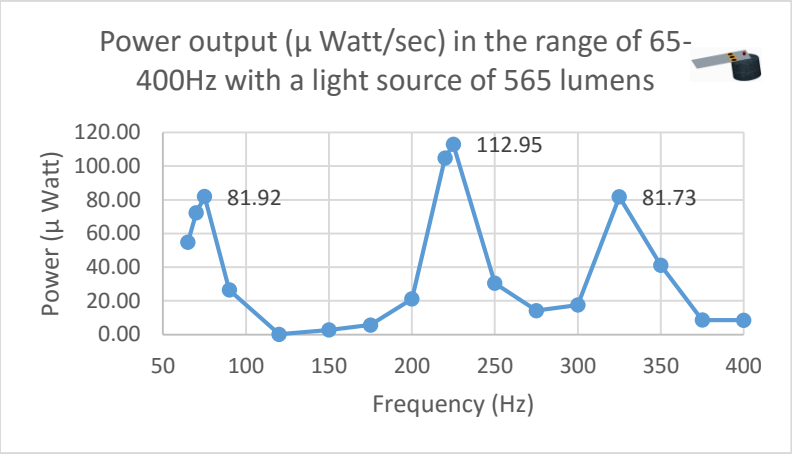

Figure 0.18 Power output of PZT with spin coated PZT with FNP 59%, ZnO 40% and epoxy 1%

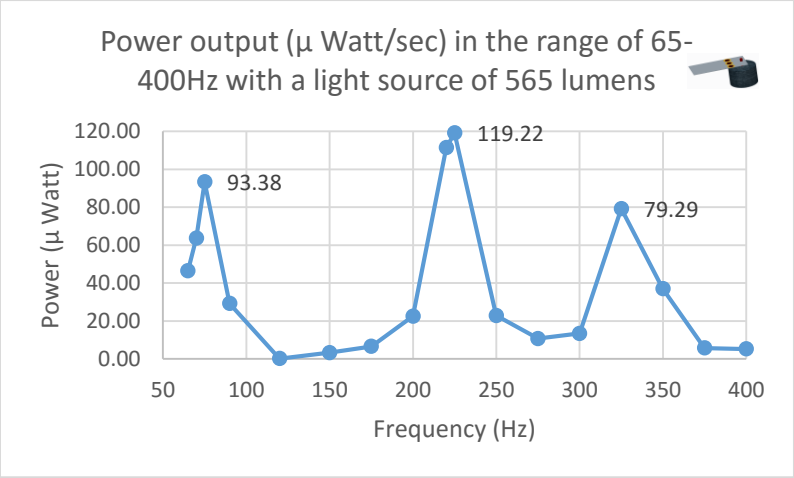

Figure 0.19 Power output of PZT with spin coated graphene 5%, FNP 54%, ZnO 40% and epoxy 1%

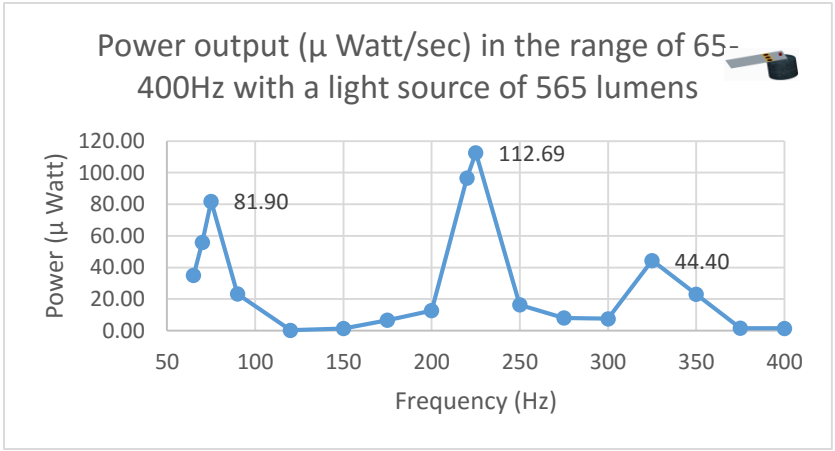

Figure 0.20 Power output of PZT with spin coated graphene 10%, FNP 49%, ZnO 40% and epoxy 1%

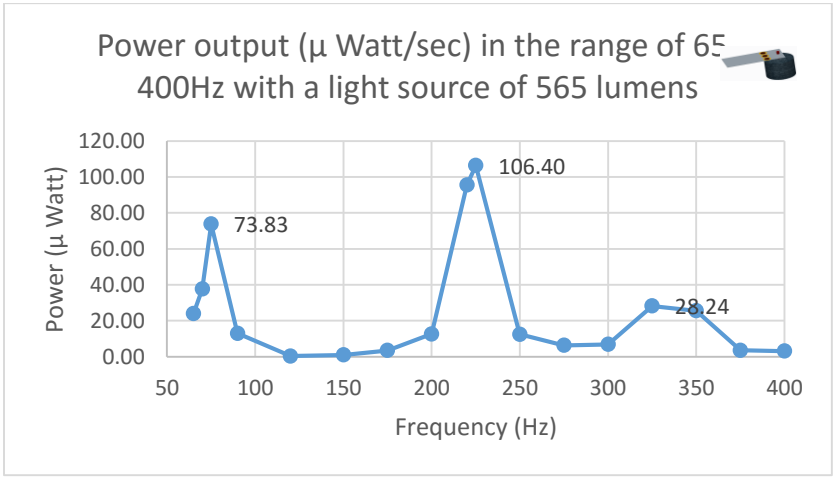

Figure 0.21 Power output of PZT with spin coated graphene 20%, FNP 39%, ZnO 40% and epoxy 1%

Results under light source of 790 lumens

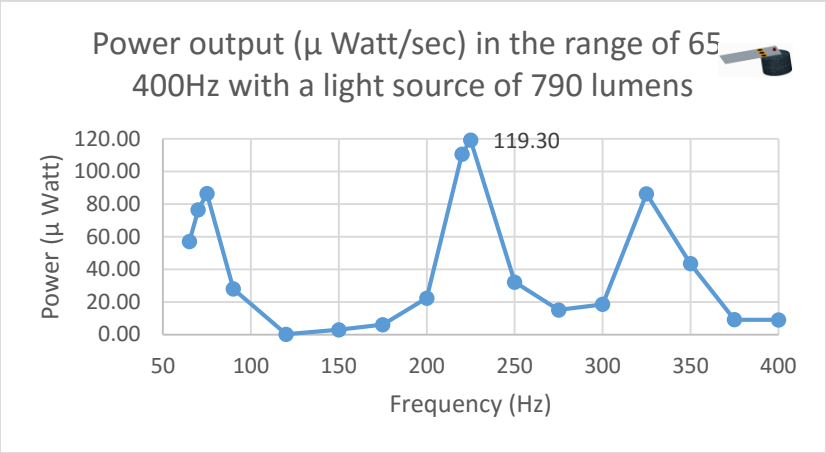

Figure 0.22 Power output of PZT with spin coated PZT with FNP 59%, ZnO 40% and epoxy 1%

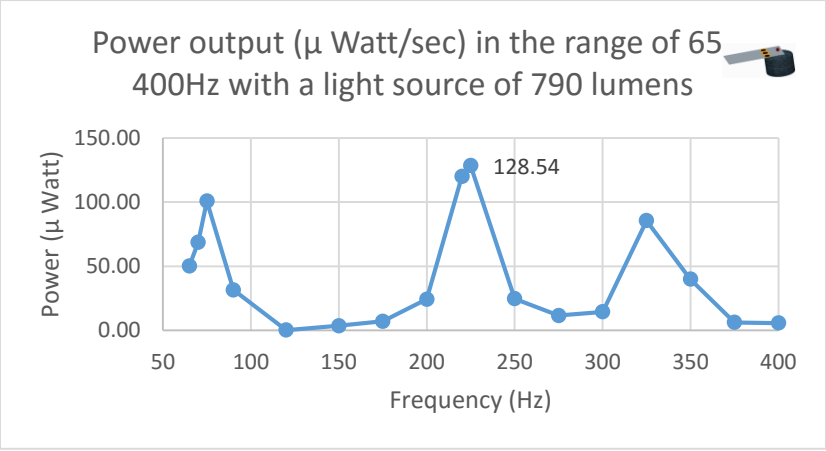

Figure 0.23 Power output of PZT with spin coated graphene 5%, FNP 54%, ZnO 40% and epoxy 1%

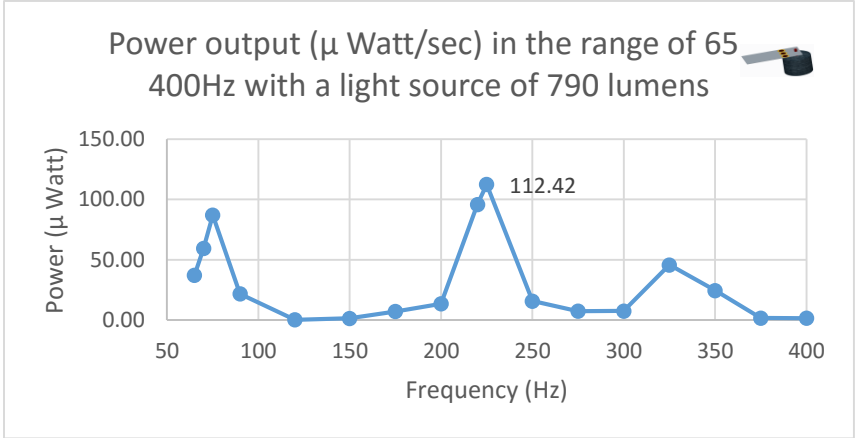

Figure 0.24 Power output of PZT with spin coated graphene 10%, FNP 49%, ZnO 40% and epoxy 1%

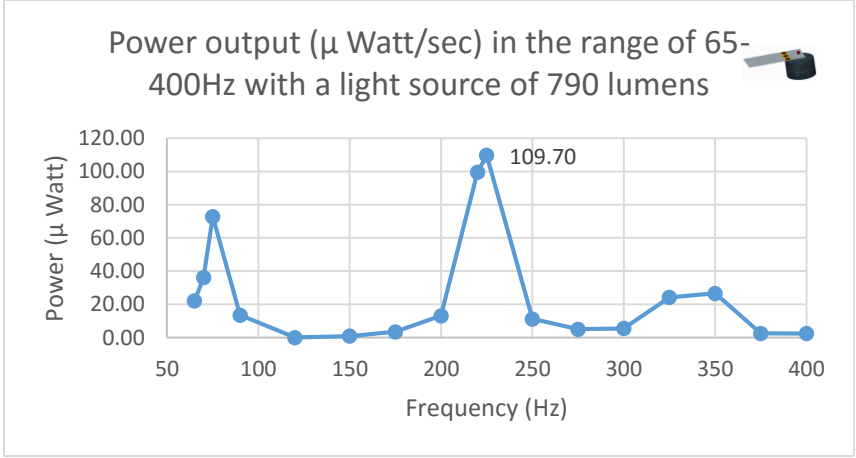

Figure 0.25 Power output of PZT with spin coated graphene 20%, FNP 39%, ZnO 40% and epoxy 1%

Results under light source of 1120 lumens

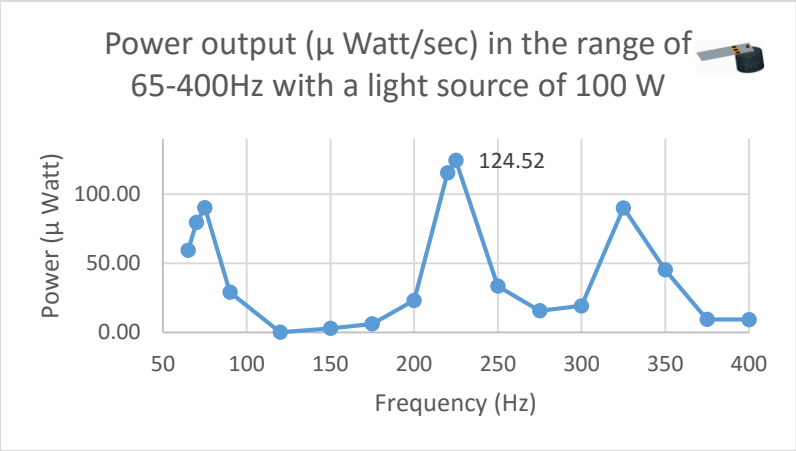

Figure 0.26 Power output of PZT with spin coated PZT with FNP 59%, ZnO 40% and epoxy 1%

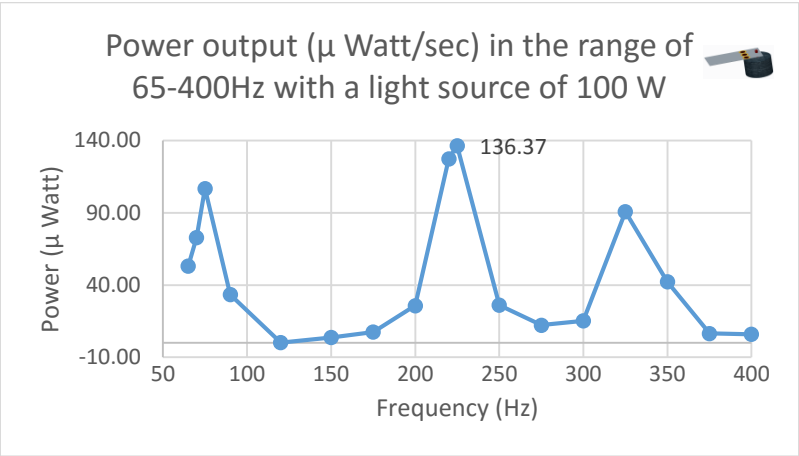

Figure 0.27 Power output of PZT with spin coated graphene 5%, FNP 54%, ZnO 40% and epoxy 1%

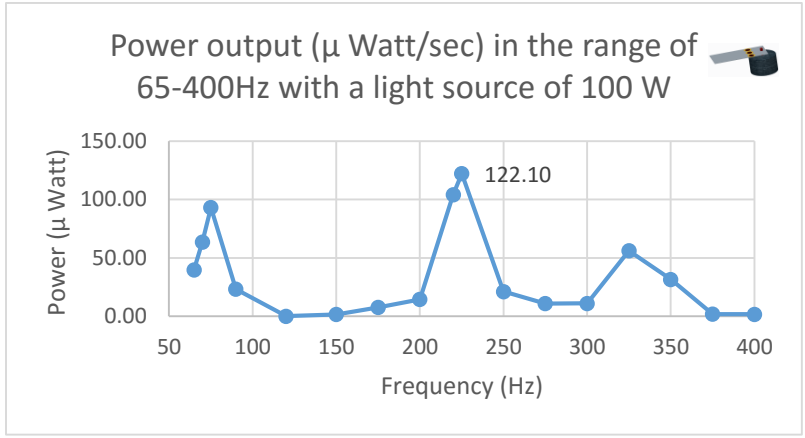

Figure 0.28 Power output of PZT with spin coated graphene 10%, FNP 49%, ZnO 40% and epoxy 1%

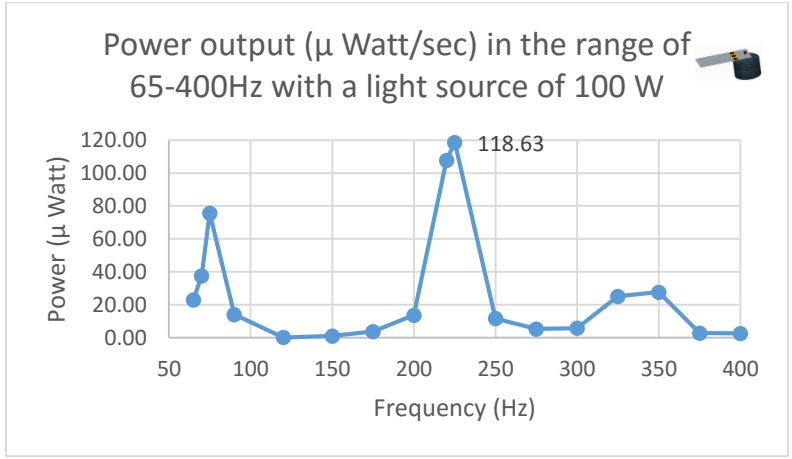

Figure 0.29 Power output of PZT with spin coated graphene 20%, FNP 39%, ZnO 40% and epoxy 1%

Results under light source of 2710 lumens

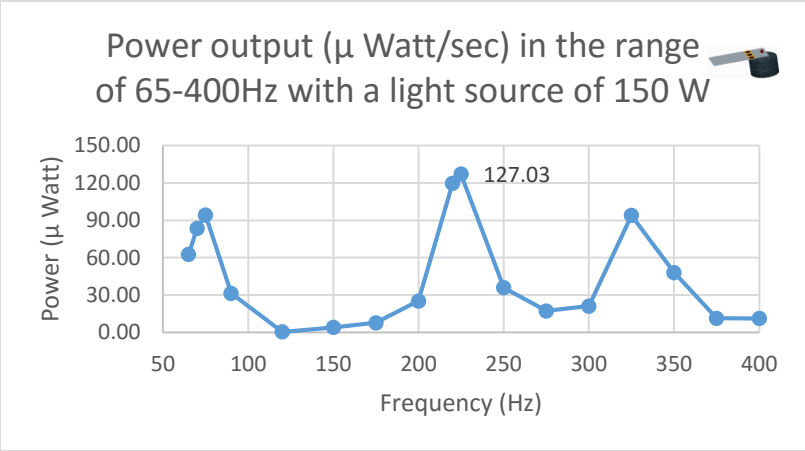

Figure 0.30 Power output of PZT with spin coated PZT with FNP 59%, ZnO 40% and epoxy 1%

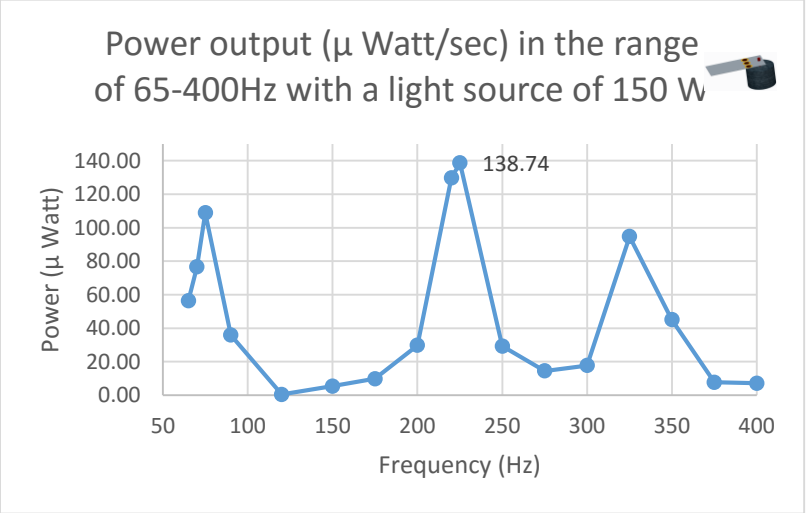

Figure 0.31Power output of PZT with spin coated graphene 5%, FNP 54%, ZnO 40% and epoxy 1%

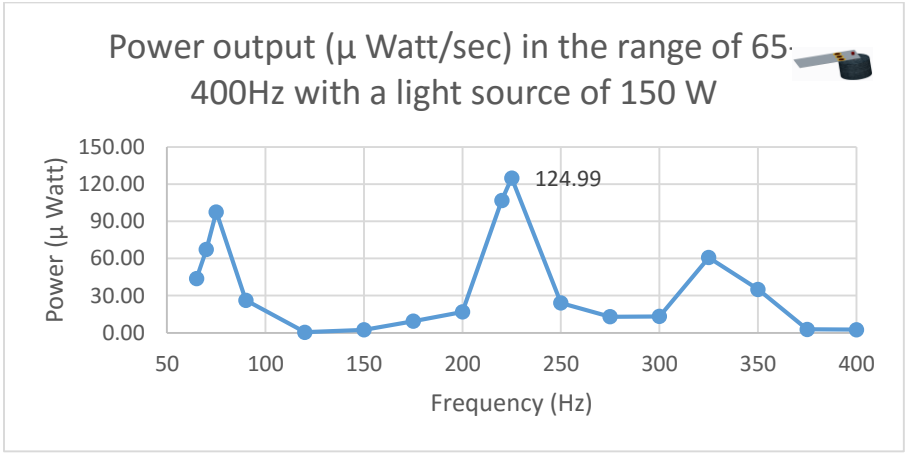

Figure 0.32 Power output of PZT with spin coated graphene 10%, FNP 49%, ZnO 40% and epoxy 1%

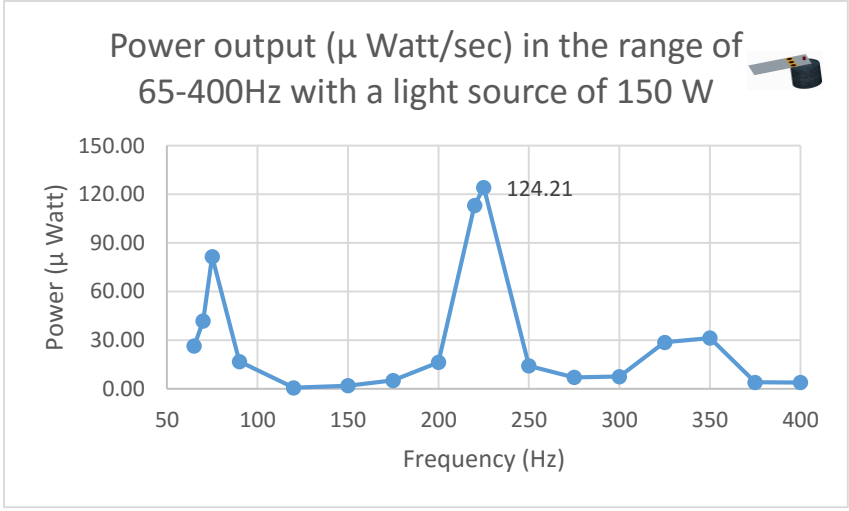

Figure 0.33 Power output of PZT with spin coated graphene 20%, FNP 39%, ZnO 40% and epoxy 1%

Results under light source of 3780 lumens

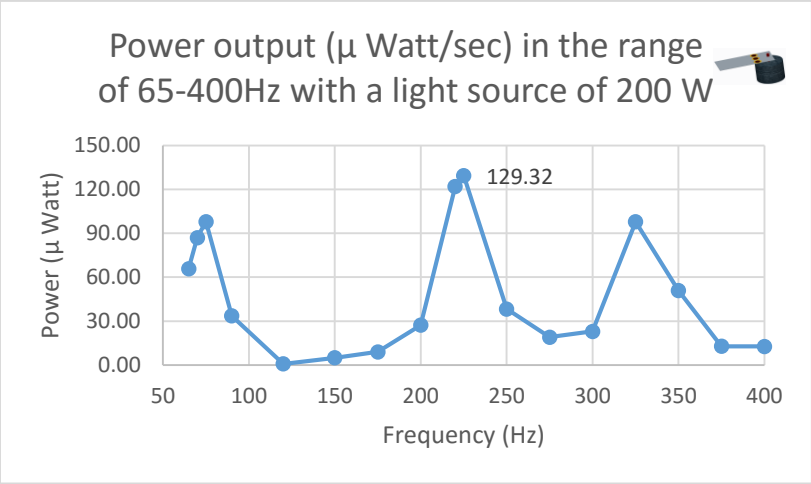

Figure 0.34 Power output of PZT with spin coated PZT with FNP 59%, ZnO 40% and epoxy 1%

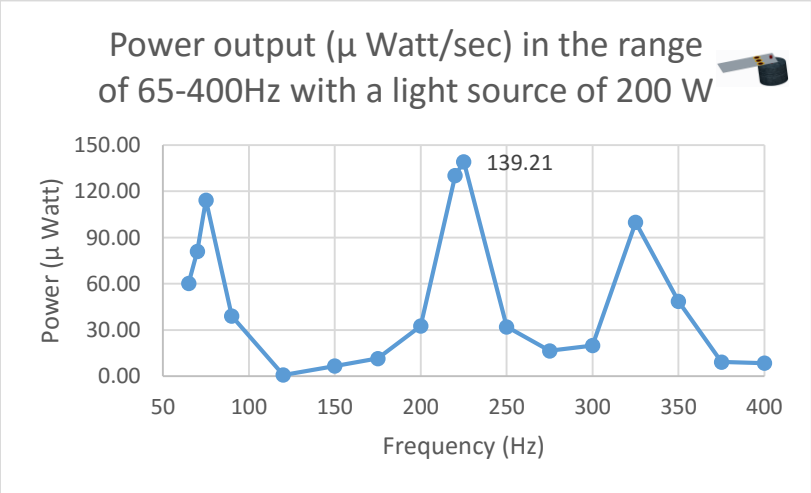

Figure 0.35 Power output of PZT with spin coated graphene 5%, FNP 54%, ZnO 40% and epoxy 1%

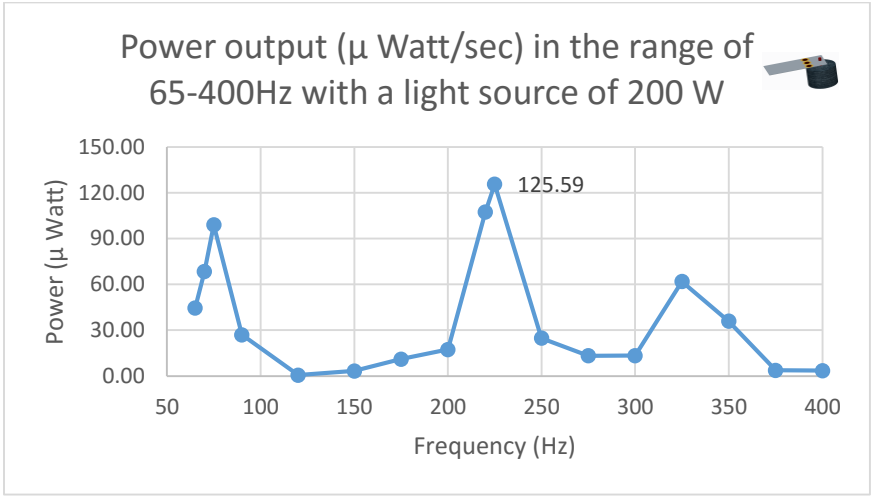

Figure 0.36 Power output of PZT with spin coated graphene 10%, FNP 49%, ZnO 40% and epoxy 1%

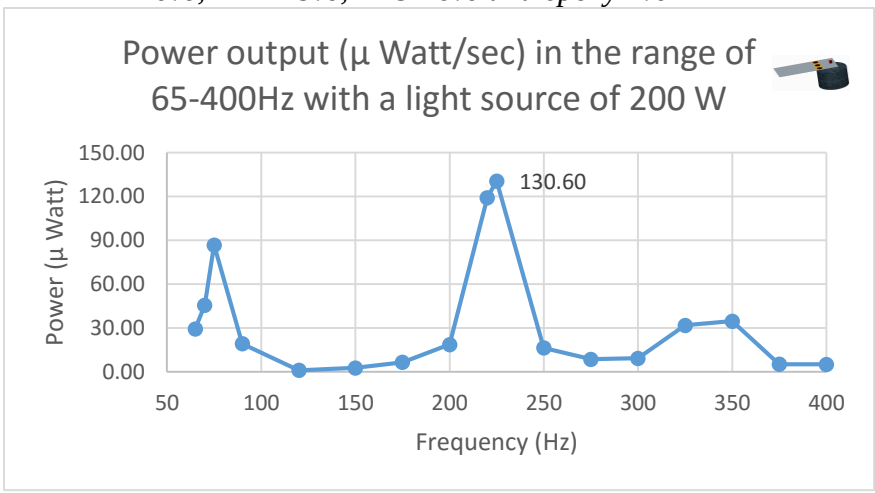

Figure 0.37 Power output of PZT with spin coated graphene 20%, FNP 39%, ZnO 40% and epoxy 1%

VITA

Abhay Sharma, son of Mr. Bijay Kumar Sharma and Dr. (Mrs.) Chandrakala Sharma, was born in Shahdol, India. He received his Bachelor of Technology (B.Tech.) degree in Metallurgical Engineering from National Institute of Technology, Raipur, India in May 2012. After his graduation he joined JSW Steel Ltd, in Bellary, India as a Graduate Engineer Trainee in Product Development and Quality Control (PDQC) Department. He attended graduate school, and obtained his Master of Science degree in Engineering Science from the Department of Mechanical Engineering at the University of Mississippi in December, 2015, while his time in University of Mississippi he worked in Jabil circuit, Memphis TN as a Planning Intern in 2015.